

A SELF-SETTING GEL SYSTEM FOR KARTOGENIN DELIVERY AND RETENTION IN CARTILAGE DEFECTS

by

JODIE MARIA HODGKINS

A thesis submitted to
University of Birmingham
for the degree of
MASTER OF SCIENCE BY RESEARCH

School of Chemical Engineering
College of Engineering and Physical Sciences
University of Birmingham

UNIVERSITY OF
BIRMINGHAM

University of Birmingham Research Archive

e-theses repository

This unpublished thesis/dissertation is copyright of the author and/or third parties. The intellectual property rights of the author or third parties in respect of this work are as defined by The Copyright Designs and Patents Act 1988 or as modified by any successor legislation.

Any use made of information contained in this thesis/dissertation must be in accordance with that legislation and must be properly acknowledged. Further distribution or reproduction in any format is prohibited without the permission of the copyright holder.

Abstract

A substantial proportion of the UK population are afflicted by cartilage damage every year, as a consequence of sporting injury or osteoarthritis. Current treatment therapies available are inadequate at providing a lasting result, while developing cell-based therapies present significant costs, resulting from strict regulations surrounding manufacturing processes. An economical solution was sought through development of an injectable bedside technology in the form of an alginate fluid gel-microenvironment and scaffold, capable of sustaining and delivering cells with chondrogenic potential, as well as retaining them during the healing process. Initial work investigated the effect of polymer concentration, with 2% gels demonstrating greater retention within model defects and superior self-setting ability. Subsequent analysis of the fluid gel microstructure revealed alignment of strands or fibres within the gel network that may influence its mechanical properties. Successful incorporation of MC3T3 fibroblast cells within alginate fluid gels was achieved, with the majority of cells expressing excellent viability over a 7-day culture period. Similar results were seen following metabolic activity analysis of BMSCs and human BMAC cells over 14-day and 21-day culture periods. Release profile studies also demonstrated steady release of KGN from the fluid gel matrix over 7 days, with no evidence of immediate burst release.

Acknowledgements

I would firstly like to express my very profound gratitude to my supervisors Professor Liam Grover, Professor Martyn Snow and Professor Lee Jeys for giving me the opportunity to work on this clinically relevant project and enabling me to join such a supportive and exciting research group. Your guidance, support and inspiration has been invaluable to me throughout my time on this project and I cannot thank you enough for the experience you have provided me. Additionally, I would like to extend a special thank you to Dr. Richard Williams, who has not only been a tremendous mentor and friend, but also provided me with ongoing encouragement and support, for which I cannot express how grateful I am to him.

Others that I would like to thank include everyone who is part of the Grover research group, as well as the supporting staff in Biochemical Engineering, including Veronica Baglin (Ronnie) and Elaine Mitchell, all of whom have helped and supported me, particularly with various laboratory equipment and techniques. Furthermore, I would like to thank other members of the academic staff at the School of Chemical Engineering including Lynn Draper and Kathleen Hynes.

I would like to acknowledge the Engineering & Physical Sciences Research Council (EPSRC) for helping to fund this project and for their financial support.

Finally, I wish to thank my family and friends, but most of all my mum, without whom none of my achievements would have been possible. Thank you for always being there for me, supporting me in everything I do and for constantly inspiring me to become the best version of myself possible.

Publications

Poster Presentations

1. "A self-setting gel system for kartogenin delivery and retention in cartilage defects", *ICRS 2016 - 13th World Congress of the International Cartilage Society*, 24th-27th September 2016, Sorrento-Naples, Italy.

CONTENTS

1	Introduction	1
1.1	Current treatment therapies	1
1.2	Alginate	3
2	Gels as platform technologies for cell therapy and drug delivery	5
2.1	Hydrogels	5
2.1.1	Range of polymers	5
2.1.2	Handling properties	6
2.2	Fluid gels	6
2.2.1	Tailoring handling properties	8
3	Bone Marrow Aspirate Concentrate (BMAC): Existing and potential methods of delivery	19
3.1	Bone Marrow Aspirate Concentrate (BMAC)	19
3.2	Existing and potential methods of delivery	21
4	Results Chapter 1: Formulation of shear-thinning gel system and cell viability within fluid gels	24
4.1	Materials and Methods	24
4.1.1	Materials	24
4.1.2	Cell culture	27
4.1.3	Fibroblast suspension within alginate fluid gels	28
4.1.4	Live/dead staining	28

4.2	Results and discussion	28
4.2.1	Characterising fluid gels in terms of their rheological profile	28
4.2.2	Tailoring formulation processing parameters for different applications .	32
4.2.3	Visualisation of the fluid gel structure	35
4.2.4	Live/dead staining of MC3T3 fibroblasts within alginate fluid gels . . .	37
4.2.5	Live/dead staining of BMAC cells	38
4.3	Concluding statement	40
5	Results Chapter 2: Tailoring release of kartogenin and the biological effects on a heterogeneous cell population within BMAC	42
5.1	Materials and Methods	42
5.1.1	Materials	42
5.1.2	Preparation of KGN fluid gel	43
5.1.3	<i>In vitro</i> release study	43
5.1.4	<i>In vitro</i> chondrogenic differentiation of rat bone marrow stromal cells .	43
5.1.5	Histology	44
5.1.6	<i>In vitro</i> chondrogenic differentiation of BM mononuclear cells	44
5.1.7	GAG contents analysis	45
5.2	Results and discussion	45
5.2.1	Sustained KGN release from 2% alginate fluid gel over 7 days	45
5.2.2	Safranin O and Alcian blue staining of rBMSC's following 14 days culture and treatment with KGN	48
5.2.3	DMMB assay and Alcian blue staining of BMAC and hBM-MSC cells following 21 days culture and treatment with KGN	49
5.3	Concluding statement	58
6	Conclusions and Future Work	60
6.1	Conclusions	60
6.2	Recommendations for future work	60

LIST OF FIGURES

1.1	Molecular configuration of sodium alginate	4
2.1	Illustration modelling the various stages of fluid gel formation, as the temperature decreases and shear forces interfere with the molecular ordering process. Molecules first associate into double helical structures or dimers through ion bridging ('w' and 'x'). Aggregation follows ('y'), reflecting an increase in viscosity (point 'C') as the temperature decreases and gel particles form. Particles may aggregate further and coalesce ('z'), resulting in the loss of 'hairy' none-ordered chain fragments from particle surfaces. A significant decrease in viscosity is observed on completion of conformational ordering of each hydrocolloid chain within gel particles ('f' and 'g') after the setting temperature is reached.	7
2.2	The 'egg-box' model illustrating cross-linking of poly(L-guluronate) chains in alginate with Ca^{2+} ions	8
2.3	The effect of cooling rate on the mechanical properties of 1% alginate fluid gels, with an initial production volume of 20ml and 0.1M CaCl_2 addition	10
2.4	Evaluation of the shear-viscosity profiles of toothpaste, glycerol and DI H_2O , when compared with 1% alginate fluid gels produced at different cooling rates .	11
2.5	The variation between the storage (G') and loss (G'') moduli of 1% alginate fluid gels at 25°C and 37°C, formulated with 0.1M CaCl_2	17

4.1	The variation between the storage (G') and loss (G'') moduli and the resulting complex viscosity of 2% alginate fluid gels at 37°C, formulated with 0.1M CaCl_2 using a temperature ramp from 60°- 25°C.	29
4.2	The variation between the storage (G') and loss (G'') moduli and the resulting complex viscosity of 2% alginate fluid gels at 37°C, (a) 24 hours post-formulation with 0.1M CaCl_2 (b) 48 hours post-formulation, using a temperature ramp from 60°- 30°C.	30
4.3	The variation between the storage (G') and loss (G'') moduli and the resulting complex viscosity of 2% alginate fluid gels at 37°C, (a) 24 hours post-formulation with 0.1M CaCl_2 (b) 48 hours post-formulation, using a peak hold ramp at 20°C and a constant shear rate of 500 s^{-1}	31
4.4	The rheological profile difference between 1% and 2% alginate fluid gels, with an initial production volume of 30ml and 0.1M CaCl_2 addition, formulated at 1.5°C cooling rate.	34
4.5	Still frames demonstrating injectable application of 2% alginate fluid gel and bead system into model cartilage defect, with alginate beads dyed red for clarity.	35
4.6	Alcian blue staining of 2% medium viscosity alginate fluid gels, formulated using (A) 60-25°C and (C) 60-30°C temperature profiles, for identification and visualisation of their microstructure on (B) glass slides.	36
4.7	Brightfield images illustrating microstructure of 2% medium viscosity alginate fluid gels stained with alcian blue and imaged on two different focal planes ((A) and (C)), overlapping in (B) (magnification x10).	37
4.8	Calcein-AM/PI live/dead staining of MC3T3 fibroblasts in 2% w/v alginate fluid gel, cross-linked with 0.1M CaCl_2 , after 7 days. Live and dead cells stain green and red, respectively, with the majority of cells remaining viable following 7 days of culture within the fluid gel matrix and no significant fibroblast death observed	38

4.9	Calcein-AM/PI live/dead staining of BMAC cells in 2% w/v alginate fluid gel, cross-linked with 0.1M CaCl ₂ , after 7 days. Live and dead cells stain green and red, respectively, with the majority of cells remaining viable following 7 days of culture within the fluid gel matrix.	40
5.1	Calibration curve of KGN concentration against absorbance at 277.8nm using UV-vis spectrophotometry.	46
5.2	Sustained KGN release from 2% alginate fluid gel over 7 days in PBS media, with continuous slow release of KGN following 24 hours.	48
5.3	Safranin O and Alcian blue staining of rBMSC's following 14 days of treatment with KGN, illustrating production of both proteoglycans and collagen, with evidence of costaining suggesting structuring of an organised matrix, particularly at 10nM.	49
5.4	Brightfield images of unstained cells indicate that the majority of BMAC cells were alive after approximately 21 days of culture. Abbreviations used: non-chondrogenic medium (CH-), chondrogenic medium (CH+), non-chondrogenic medium supplemented with 100 nM (100nM), 200 nM (200nM) or 400 nM (400nM) of KGN (dissolved in DMSO and further diluted using non-chondrogenic medium).	51
5.5	Brightfield images of unstained cells indicate that the majority of hBM-MSC cells were alive after approximately 21 days of culture. Abbreviations used: non-chondrogenic medium (CH-), chondrogenic medium (CH+), non-chondrogenic medium supplemented with 100 nM (100nM), 200 nM (200nM) or 400 nM (400nM) of KGN (dissolved in DMSO and further diluted using non-chondrogenic medium).	52
5.6	DMMB assay results following the treatment of hBM-MSCs and BMAC with 100nM of KGN over 21 days.	53
5.7	DMMB assay results following the treatment of hBM-MSCs and BMAC with 200nM of KGN over 21 days.	53

5.8	DMMB assay results following the treatment of hBM-MSCs and BMAC with 400nM of KGN over 21 days.	54
5.9	DMMB assay results following the treatment of hBM-MSCs with varying concentrations of KGN over 21 days. Abbreviations used: non-chondrogenic medium (CH-), chondrogenic medium (CH+), non-chondrogenic medium supplemented with 100 nM (100nM), 200 nM (200nM) or 400 nM (400nM) of KGN (dissolved in DMSO and further diluted using non-chondrogenic medium).	55
5.10	DMMB assay results following the treatment of BMAC with varying concentrations of KGN over 21 days. Abbreviations used: non-chondrogenic medium (CH-), chondrogenic medium (CH+), non-chondrogenic medium supplemented with 100 nM (100nM), 200 nM (200nM) or 400 nM (400nM) of KGN (dissolved in DMSO and further diluted using non-chondrogenic medium).	56
5.11	Alcian blue staining of proteoglycans produced by BMAC and hBM-MSC cells. Abbreviations used: non-chondrogenic medium (CH-), chondrogenic medium (CH+), non-chondrogenic medium supplemented with 100 nM (100nM), 200 nM (200nM) or 400 nM (400nM) of KGN (dissolved in DMSO and further diluted using non-chondrogenic medium).	57

CHAPTER 1

INTRODUCTION

Cartilage damage is a common occurrence, particularly amongst younger populations, with approximately 10,000 people in the UK seeking treatment for this disorder each year [1, 2]. Forgoing treatment could result in chronic pain and the development of osteoarthritis, which presents a significant economic burden due to the cost of treatment and impact of disability [3]. Articular cartilage is designed to enable the smooth mobility of joints and protection of subchondral bone from impact and stress [4]. It is composed of hyaline cartilage in the form of an extracellular matrix, which contains a sparsely distributed population of chondrocyte cells amongst other constituents including collagen, proteoglycans and water. The most abundant type of collagen present is type II (90-95%), which is arranged into fibrils and fibers entangled with proteoglycans. There are a range of proteoglycans present in articular cartilage, such as aggrecan, biglycan and decorin, but aggrecan is present in the largest quantities and is able to form proteoglycan aggregates with hyaluronan [5]. Unfortunately, articular cartilage is avascular in nature, which limits its ability for repair or regeneration. Therefore, if damage does occur, scar tissue is formed from the subchondral bone, which lacks type II collagen and contains different proteoglycans, resulting in a weaker biomechanical structure [1].

1.1 Current treatment therapies

There are currently a number of treatment therapies available for chondral lesions, including microfracture, osteochondral allografts and autologous chondrocyte implantation (ACI). However, none of these have yet been able to offer a long-term durable solution [1, 4]. Whilst microfracture enables the release of bone marrow stem cells (BMSCs) by perforating the subchondral

bone, it results in the formation of fibrocartilage, which is mechanically inferior to hyaline cartilage and contains a larger amount of type I collagen [6]. Additionally, osteochondral allografts, despite demonstrating feasible transplantation of chondrocytes from cadavers without creating an immunological response, present possible risks of disease transmission and supply is unlikely to meet the overall demand for replacement tissue in a resource efficient manner. [1, 6]. ACI is one of the more recently developed cell-based treatment strategies, where autologous chondrocytes are first collected and expanded through cell culture, before being reimplanted beneath a periosteal patch [6]. However, studies have revealed that the cells can undergo a change in phenotype during expansion, diminishing their ability to form type II collagen [1, 7]. The treatment cost is also extremely expensive (around £25,000) and, due to a lack of clinical evidence of a substantial cost-benefit gain as reviewed by the National Institute for Health and Care Excellence (NICE), there are a limited number of hospitals offering this procedure [8].

An alternative option for therapy that has demonstrated comparable efficacy to ACI, is the use of BMSCs with chondrogenic potential, which have improved proliferation rates compared to chondrocytes and, importantly, permit greater control over differentiation to (and maintenance of) a chondrogenic phenotype. They have also exhibited great potential in improving quality of life in older population groups (over 45 years of age), where ACI has been less effective [9]. However, extensive manipulation of cells, such as cell expansion (culture), results in their classification as an Advanced Therapy Medicinal Product (ATMP) by the European Medicines Agency [10]. Such processes require production under Good Manufacturing Practice (GMP) conditions, which has associated costs in terms of investment and labour that decrease the probability of acceptance by the National Institute for Clinical Excellence (NICE), and thus the feasibility of the treatment being implemented by national health service providers [11, 12].

The aim of this project was to provide an economical solution to aid articular cartilage damage in the form of a bedside technology, which is capable of sustaining cells of chondrogenic potential and delivering them to the defect site whilst retaining the cell population during the healing

process. The gel system will therefore need to provide the correct biochemical microenvironment to direct their lineage down a chondrogenic route. Consequently, a recently discovered, small nonprotein molecule kartogenin (KGN), that has been shown to stimulate selective differentiation of stem cells into chondrocytes, could facilitate the differentiation of progenitor cells when incorporated into the fluid gel microenvironment [13, 14]. The objective with this approach is to make more effective use of cell-based therapies by providing a mechanism of delivery and retention of both the cell population and the biochemical environment (the cell 'niche') required to direct cell fate, and thus maximise the chance of achieving successful regeneration of the affected tissue.

There has continually been significant interest in the application of gels formulated using a range of synthetic and biological polymers in tissue engineering and specifically, for cartilage repair and regeneration [15, 16]. This stems from their numerous desirable properties that include excellent biocompatibility and similitude to the extracellular matrix (ECM) of biological tissues [16]. Although various biopolymers can be used to create gels, including agarose and κ -carrageenan, for this work two different grades of sodium alginate were chosen, due to its resistance to thermo-reversible effects which κ -carrageenan, agar and gellan are impartial to [17, 18]. Alginate was also chosen due to its ease of chemical modification and suitability for use as a biomaterial, particularly for introducing cell selectivity attributes [19].

1.2 Alginate

Commercially, alginates are currently extracted from marine brown algae, where they provide a structural function as a gel in the intracellular matrix [20]. From Figure 1.1, it can be seen that the sodium alginate structure consists of a sequence of 1,4-linked α -L-guluronic acid (G) and β -D-mannuronic acid (M) residues, which are covalently linked and organised into blocks of recurring MM and GG residues, as well as hybrid blocks of MG residues [21, 22]. This sequence and composition will differ according to the type and source of the alginate being

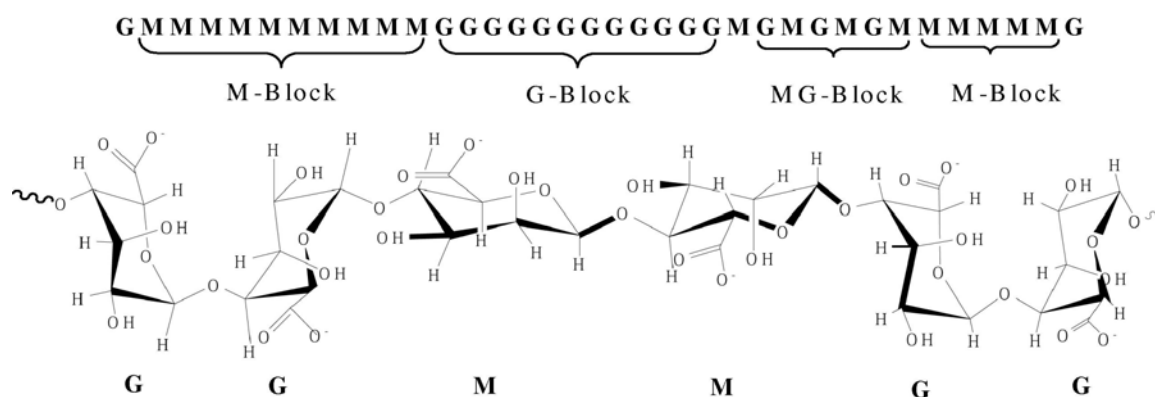


Figure 1.1: Molecular configuration of sodium alginate [21].

used [19, 22]. Gelation of alginates can occur through cross-linking of the alginate structure by divalent cations, typically Ca^{2+} . This can either take place internally, utilising an insoluble source of calcium e.g. CaCO_3 , or externally through diffusion of soluble calcium ions e.g. CaCl_2 into the alginate solution [22]. The ease of chemical modifying alginate is attributed to the availability of carboxyl and hydroxyl groups present across the polymer backbone [21].

In this thesis, the potential of an alginate fluid gel as a suitable delivery matrix and scaffold has been explored, which would be capable of flowing under shear (enabling parenteral administration) and 'setting' *in situ* upon removal of shear forces. The definition of 'setting', in this context, refers to a range of viscosity values which give the gel shape maintaining properties and result in it ceasing to flow. Therefore, this 'setting' mechanism would not require use of any additional chemical agents and the gel materials used have already gained FDA/EMA approval, thus allowing regulatory approval to be obtained more easily. The delivery matrix must also be capable of maintaining the viability of a suitable cell population that has chondrogenic potential, as well as possessing a desirable rate of degradability to ensure cells are retained at the defect site following delivery. Here, they would then ideally facilitate chondral repair and regeneration through the production of anti-inflammatory molecules and ECM secretion.

CHAPTER 2

GELS AS PLATFORM TECHNOLOGIES FOR CELL THERAPY AND DRUG DELIVERY

2.1 Hydrogels

Hydrophilic gels, also known as hydrogels or quiescent gels, are structured through the physical or chemical cross-linking of hydrophilic polymers in the presence of an aqueous solvent, such as water, which occupies the voids between the polymeric junctions or chain entanglements, thus creating a three-dimensional, insoluble network [23, 24]. Hydrogels are classified as homo-, co- or multi-polymeric, depending on the number of monomer species utilised in the reaction. They can also be categorised according to their physical form, for example as a microsphere, matrix or film, which is a result of the polymerisation preparation technique [25, 26, 27, 28, 29].

As previously mentioned, hydrogels can vary depending on the type of cross-linking mechanism. This inherently affects their properties, as permanent junctions are formed by chemically cross-linked polymer chains, whereas transient junctions are established through physical cross-linking, including hydrogen bonds, ionic interactions and entanglements of polymer chains. Therefore, further classification of hydrogels can be made according to the electrical charge present on the polymer chains, which could be ionic, amphoteric, zwitterionic or neutral [30].

2.1.1 Range of polymers

Hydrogels can be formulated from a wide variety of polymers of synthetic or natural origin, or even a combination of each. The advantage of synthetic polymers, e.g. poly(vinyl alcohol)

(PVA) or poly(ethylene glycol) (PEG), is their definitive structure allowing modifications to be made, such as adjusting their degradability or chemical and biological activity. They also demonstrate good stability in fluctuating temperatures and have a significant water absorption capacity, which may be as a result of their superior gel strength. However, natural polymers are highly biocompatible and can be sourced from polypeptides or polysaccharides, e.g. hyaluronic acid, collagen, or alginate, indicating their wide abundance and favourable biodegradation products, in terms of saccharide or amino acid constituents [27, 28].

2.1.2 Handling properties

When subjected to sufficient stress, hydrogels display impressive elastic behaviour, similar to that of natural rubbers. Upon applying a minor deformation to less than one fifth of its structure, a hydrogel is capable of quickly regaining its initial dimension, despite typically being described as 'soft' materials, as their elastic moduli approximately ranges from kPa to MPa [25, 26]. This illustrates one of the limitations of hydrogels as their inferior mechanical strength, which affects their overall handling properties [23, 29, 30, 31].

2.2 Fluid gels

Fluid gels consist of a suspension of coagulated particles, formed from a biopolymer solution undergoing shear forces in a gelling environment [17, 18]. These shear forces are believed to disrupt the molecular ordering process, thereby limiting the number and length of helices formed and producing a gel that displays shear thinning behaviour. [32, 33] This is portrayed in Figure 2.1, where molecules first associate into double helical structures or dimers through ion bridging (represented by both 'w' and 'x'), which, as in the case of alginate, later results in egg box formation.

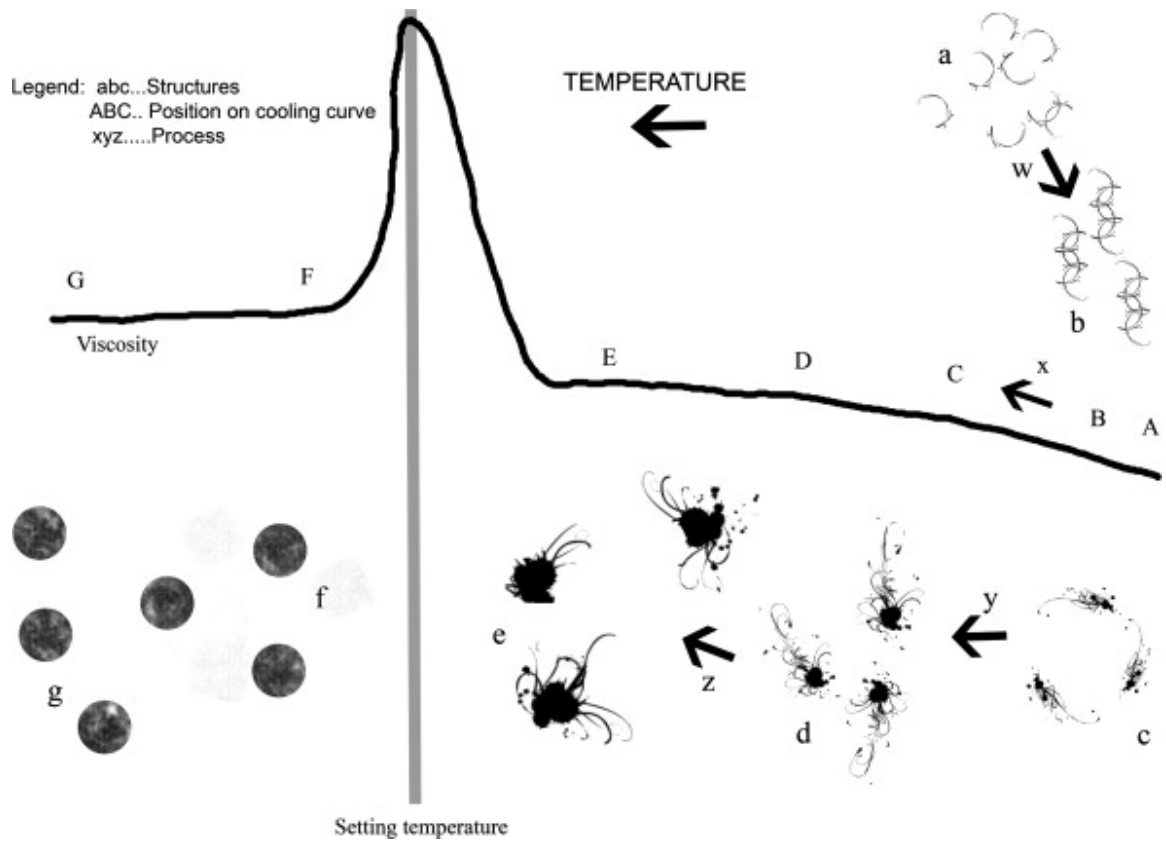


Figure 2.1: Illustration modelling the various stages of fluid gel formation, as the temperature decreases and shear forces interfere with the molecular ordering process. Molecules first associate into double helical structures or dimers through ion bridging ('w' and 'x'). Aggregation follows ('y'), reflecting an increase in viscosity (point 'C') as the temperature decreases and gel particles form. Particles may aggregate further and coalesce ('z'), resulting in loss of 'hairy' none-ordered chain fragments from particle surfaces. A significant decrease in viscosity is observed on completion of conformational ordering of each hydrocolloid chain within gel particles ('f' and 'g') after the setting temperature is reached [34].

As presented in Figure 2.2, the gelation of alginates can be described by the 'egg-box' model and demonstrates how cations are able to effectively cross-link the alginate structure by embedding into the crevices created through dimerisation.[34, 35] These structures then begin to aggregate (denoted by 'y'), reflecting an increase in viscosity (at point 'C') as the temperature decreases and gel particles are formed. These particles may aggregate further and coalesce (indicated by 'z'), resulting in loss of 'hairy' none-ordered chain fragments from particle surfaces. However, as previously mentioned, this process will be limited by the magnitude of the shear field applied to the system, thus determining the final size of the gel particles. After the setting

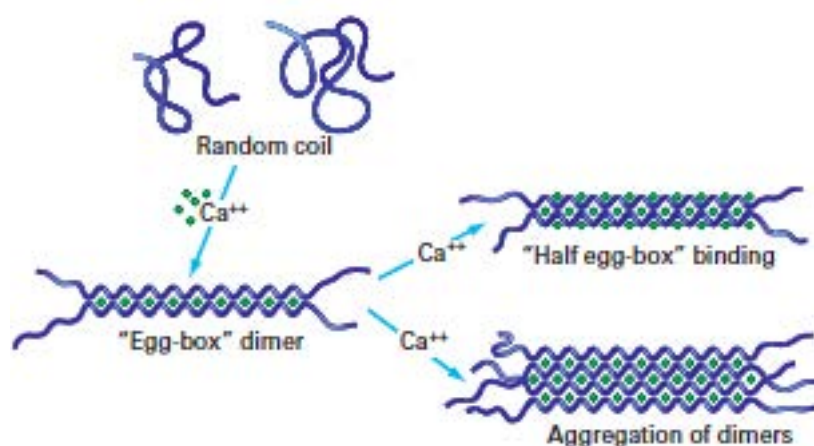


Figure 2.2: The ‘egg-box’ model illustrating cross-linking of poly(L-guluronate) chains in alginate with Ca^{2+} ions [35].

temperature has been reached, a significant decrease in viscosity can be observed, which is a consequence of completion of the conformational ordering of each hydrocolloid chain within the gel particles (illustrated by ‘f’ and ‘g’).[34] Therefore, the key formulation parameters for fluid gels include the rate of shear, cooling and divalent ion addition. Previous work by Streather focused upon screening a large range of each of these parameters to determine which had the greatest influence on the fluid gel mechanics.[36] This previous work identified a combination of parameters that may produce an injectable formulation, that is shape maintaining upon application and subsequent work has systematically refined those parameter values, with particular attention to the variation of cooling rate. Furthermore, the possibility of increasing production volume of fluid gels has been explored, in addition to the potential impact of incorporating a solid phase within a fluid gel, in the form of alginate gel beads [37].

2.2.1 Tailoring handling properties

Viscosity

One of the key fluid-gel formulation parameters is the cooling rate, as this can greatly influence the rheological properties of the fluid gel. This has been illustrated in previous work, which analysed the effect of cooling rate on the viscosity of alginate fluid gels, whilst maintaining

a constant shear rate (450s^{-1}) [37]. However, there was insufficient control over the addition of the cross-linking agent, calcium chloride, which is a limiting factor. Earlier studies have demonstrated improved reproducibility of fluid gels produced at higher shear rates of 450s^{-1} and 700s^{-1} , whereas lower shear rates (200s^{-1}) can generate inhomogeneous fluid gels and have greater variability [36]. The findings revealed that fluid gels cooled at slower cooling rates ($0.25^{\circ}\text{C min}^{-1}$) were associated with lower shear-viscosity profiles (Fig. 2.3), which has been suggested are an effect of smaller fluid gel particulates formed at reduced cooling rates, as the shear rate dominates the formulation process. Similarly, increasing the cooling rate results in formation of larger gel particulates, as illustrated in Fig. 2.3 by the higher shear-viscosity profiles of fluid gels formulated at faster cooling rates [34, 37]. Although, additional work by Gabriele *et al.* found that decreased cooling rates moderately increased the viscosity of κ -carrageenan fluid gels, which they attributed to more substantial bridging of gel particulates, as they have more time to develop. They also discovered that the structure of fluid gels is subject to additional "strengthening" post-formulation and occurs most prominently in gels produced at faster cooling rates. However, the sample volumes ($1250\mu\text{L}$) studied and lower shear rates (50s^{-1} , 100s^{-1} and 300s^{-1}) used to manufacture the fluid gels limited the significance of the study [37, 38].

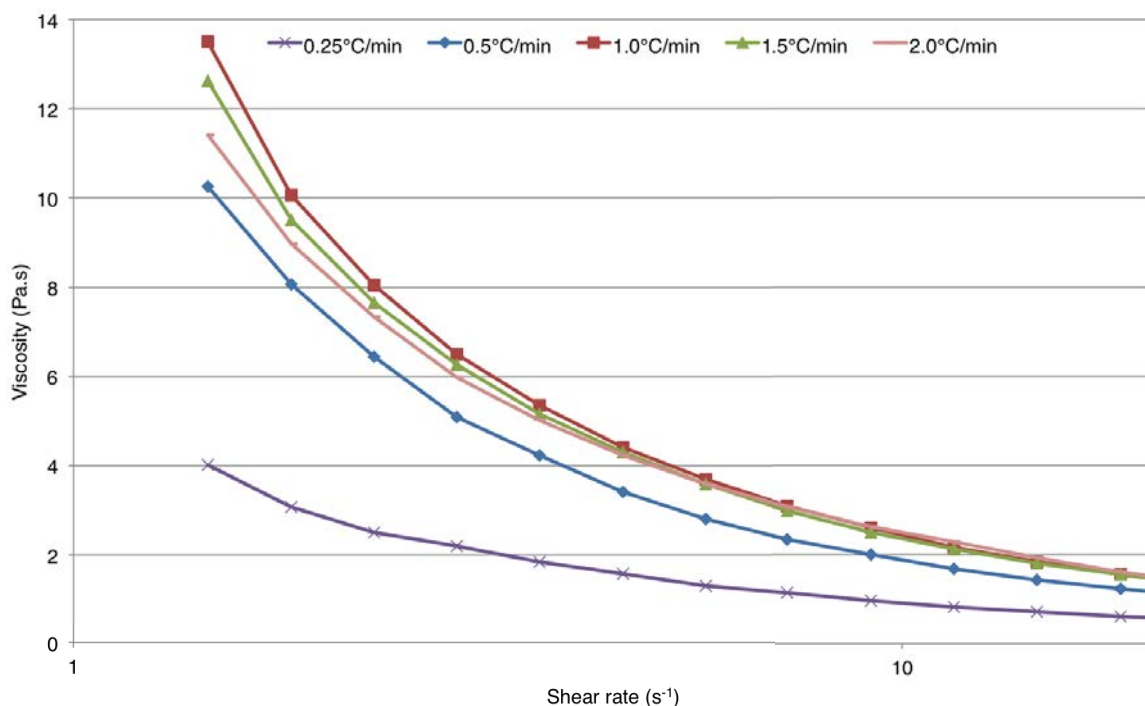


Figure 2.3: The effect of cooling rate on the mechanical properties of 1% alginate fluid gels, with an initial production volume of 20ml and 0.1M CaCl_2 addition [37].

In order to put the shear-viscosity response of alginate fluid gels, cooled at varying rates, into context, they were compared to those of deionised water ($\text{DI H}_2\text{O}$), glycerol and toothpaste (Fig. 2.4). This helped illustrate the shear thinning behaviour of toothpaste, though at significantly higher measured values of viscosity than those evaluated for fluid gels produced at the specified cooling rates.

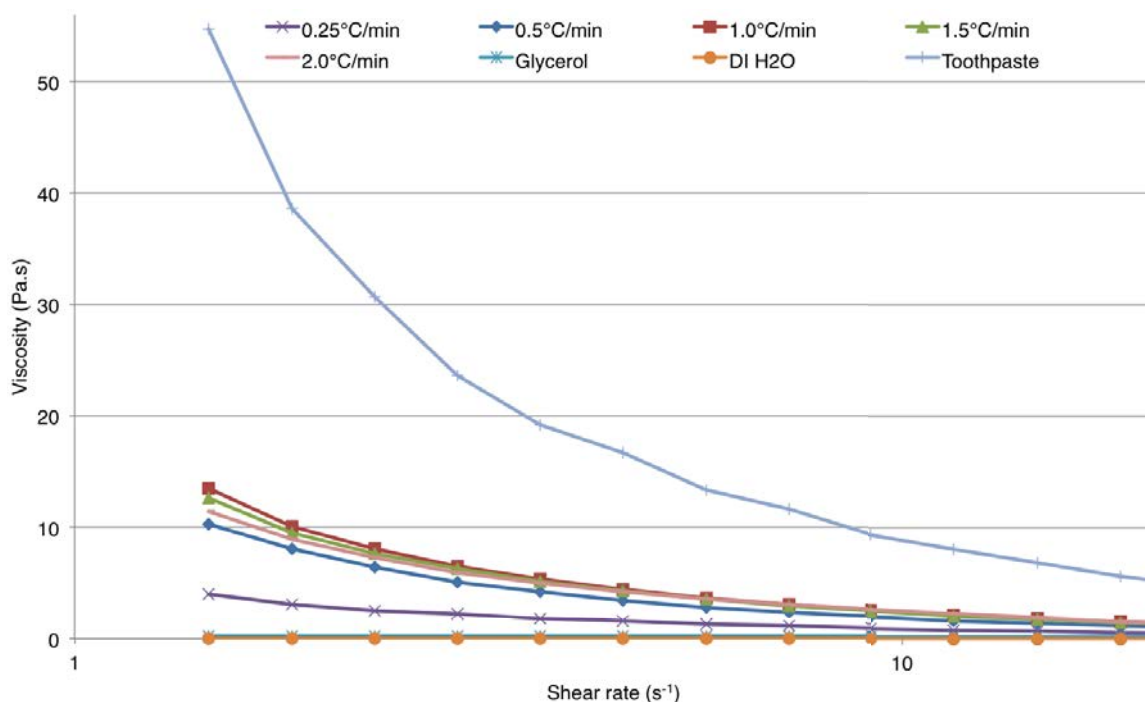


Figure 2.4: Evaluation of the shear-viscosity profiles of toothpaste, glycerol and DI H₂O, when compared with 1% alginate fluid gels produced at different cooling rates [37].

Biodegradability

Experimental studies on the biodegradability of gels have been carried out since 1947, where initial work on alginate dressings by Blaine revealed its complete absorption by animal tissues, which was dependent upon the concentration of the cross linking agent, such as calcium chloride, or the sodium alginate concentration (3% and 5%). Additionally, the physical structure and form of the gel also had an influence on its rate of absorption, though overall the immune response was negligible [39]. Subsequent work determined that the vascularity of the tissue affected the rate of absorption as well, and alginates with synthetically increased sodium ion content were absorbed much more quickly than those with higher calcium ion content [40]. This is in agreement with more recent findings investigating the distribution of alginate-tyrosinamide in male Wistar rats, following systemic and subcutaneous administration, which indicated the dependence on polymer molecular weight, as fractions of low molecular weight ($\leq 48,000$ counts per minute) were removed in the urine, whilst fractions of larger molecular weight resided in

the circulatory system, but without any tissue accumulation. This was suggested to result from the ability of the former to attain clearance by the lymphatic system and furthermore, delivery subcutaneously ensured approximately 70% retention at the application site [41]. There are also fewer reaction locations in higher molecular weight polymers, limiting the opportunity for hydrolysis and reducing the rate at which degradation can take place [42].

These preliminary investigations were crucial for the development of the alginate fibre dressing, Sorbsan, which easily undergoes biodegradation in wounds, so that removal is unnecessary and allows granulation tissue to be formed. This product has demonstrated successful application in treating trophic and diabetic ulcers that can become infected and inflamed, thus prolonging the healing process [43]. Thereafter, it was shown to minimise blood loss at skin graft donor sites, indicating considerable haemostat efficacy. These biodegradable properties of calcium alginate are attributed to its conversion into sodium alginate, thereby inhibiting the accumulation of residual material in the wound due to its solubility in bodily fluids [44, 45]. Similar observations were made by Stoichet et al., who studied the stability of cell-encapsulating alginate and agarose hydrogels *in vitro*. Their work illustrated a reduction in the strength of alginate gel over a 3-week period, implicating the diffusion of calcium ions from the matrix and causing decrosslinking of the structure. This allowed improved permeation of ovalbumin and BSA and highlighted the importance of controlling biodegradation, particularly for gels that require mechanical functionality, such as those intended for use in orthopaedic implants [46]. Ideally, it would be desirable to tailor the rate of polymer degradation in parallel with the rate of tissue growth, which has led the examination of appropriate methods and techniques that can help achieve this [15]. These include periodate oxidation of biopolymers, such as sodium alginate, which, following incorporation with chondrocyte cells, enabled the formation of new cartilage-like tissue in SCID mice. In comparison to unmodified alginate, its partially oxidised configuration improved its biodegradability *in vivo* over 7 weeks, whereas localised regions of cartilage like-tissue growth appeared to be restricted by substantial amounts of unmodified alginate residue, which they reported was consistent with previous findings [47]. In addition to

periodate oxidation, other alternative procedures that can enhance the rate of biodegradation include irradiation or utilisation of the enzyme, alginate lyase, which respectively cleave covalent and glycosidic bonds throughout the polymer. These have both been employed in the formulation of a biodegradable alginate matrix for the encapsulation of isolated ovarian cells, which were successfully implemented *in vitro* and *in vivo*. However, prior to this, they noticed no difference in the rigidity or size of untreated alginate beads, following one week of *in vitro* culture with isolated preantral follicles. Therefore, they were able to conclude that the biodegradation of the alginate scaffold enabled the infiltration of cells and vascularisation *in vivo*, potentially promoting the expansion and longevity of the encapsulated ovarian cells. This has promising applications for restoring endocrine activity and fertility in cancer patients, where, after disease remission, transplantation of cryopreserved ovarian tissue is not advised, so the development of a biodegradable artificial ovary could enable survival and growth of isolated follicles and ovarian cells [42, 48, 49, 50]. Analogous results were also described in earlier literature by Alsberg et al. and Simmons et al., who analysed the effects of alginate hydrogel scaffold degradation on the formation of bone tissue. Using γ -irradiation, they were able to regulate the biodegradability of alginate, with irradiated samples supporting faster synthesis of mechanically superior osseous tissue. As previously mentioned, this has been confirmed to occur from an accelerated transfer of divalent calcium ions with monovalent cations, including potassium, phosphate and sodium, which may be distributed throughout the medium encompassing the alginate hydrogel. Remarkably, alginate gel samples used to encapsulate fibroblast cells were able to maintain their shape and self-supporting structure over a 4-week period, despite experiencing an increased degradation rate over the first week [51]. These studies also helped to determine sufficient levels of radiation dosage, as it is crucial that biopolymers undergo degradation at an appropriate rate that can still sustain cell proliferation and provide support in vacuous defects [49, 52, 53]. Another process that has been utilised for enhanced biodegradability is adjustment of the molecular weight distribution in alginate polymer chains, which preserved the mechanical behaviour and elastic moduli of gels, as well as facilitate bone growth through the delivery and stimulation of bone marrow stromal cells (BMSCs). This was accomplished through oxida-

tion with sodium periodate and γ -irradiation in order to modify the chemical composition and molecular weight of alginates with different molecular weights [54, 55].

Comparatively, studies have examined the biodegradable properties of gellan gum, specifically demonstrating its capability *in vitro*. Results from work by Lee et al., suggested that the acyl content may influence its degradation, as low acyl gellan gum displayed greater stability than blends of low/high acyl gellan gum, with higher ratios of high acyl gellan gum exhibiting faster rates of degradation. They theorised that the presence of a large acyl group on the 1,3- β -D-glucose might limit the configuration of tightly bound helices and hence, affect the gel stability. Therefore, they concluded that applications of low acyl gellan gum (2% w/v) may be suitable for musculoskeletal tissue regeneration, allowing matrix reconstruction to transpire over longer periods of time and also, considering its superior compressive modulus [56]. Additional experiments have measured the degradability of low acyl gellan gum (1% w/v) against other potential biopolymers, sodium alginate (2% w/v) and low methoxy (LM) pectin (2% w/v), following seeding with rat BMSCs. Interestingly, the data showed great variations between each polysaccharide, particularly for the alginate hydrogels, which degraded to 20% of their original modulus by day 7, whereas gellan gel hydrogels took over 28 days to reach this value. This was explained, as previously mentioned, due to the initial exchange of critical ions and restructuring of the alginate gel matrix, after which there is a decrease in the rate of degradation. Furthermore, deposition of mineral by differentiated rBMSCs may have induced calcium chelation, known to originate from organic phosphate components. However, the validity of this research is applicable to low viscosity (20-40 cps) sodium alginate and gel testing is limited to its relevance *in vitro* [57, 58]. It appears that there is insufficient evidence surrounding the degradability of gellan gum *in vivo*, although some preliminary investigations have been made, they have declared the need for further analysis to gain an understanding of its mechanism of degradation [59, 60].

pH response

Another factor that can influence the biodegradability of polymeric hydrogels is the pH of the environment, which varies depending on the location of the tissue within the body and also, on whether it is in a healthy or diseased condition. For example, the stomach features the most acidic domain, with a pH range of 1.0 to 3.0, whilst the pH of a wound or inflamed tissue can fluctuate from as much as 5.45 to 8.65. This can significantly impact the structure and integrity of a gel, as it is inclined to swell when exposed to a pH less than or greater than its pK_a value, dependent upon the cationic or ionic nature of the polymer, respectively. These mechanical properties have so far been exploited in the field of drug delivery, as they offer considerable advantages for targeted therapies, including treatment for intestinal diseases or malignant tumours. Specifically, protein molecules, such as insulin, have been incorporated into hydrogel networks, utilising the polycationic copolymer, chitosan, with a pK_a of approximately 6.3. This would therefore enable oral delivery of insulin, as the hydrogel structure would be maintained and hence, protect the therapeutic protein until it passed into the stomach, where the amino groups on the polymer chain would then become ionised, causing electrostatic repulsion. Consequently, the hydrogel would become swollen, creating a more porous network and also, allowing the insulin to elute out into the surrounding environment [25, 61, 62, 63, 64]. In addition to this, this technology has also exhibited its anticancer therapeutic potential, as extracellular tumours can be distinguished by their slightly acidic climate (pH 6.5-7.2) [61, 63, 65].

Until recently, the focus of this work had centred around quiescent gels, but current examination by Bradbeer et al. has explored the effects of subjecting low acyl gellan gum fluid gels to a selection of acidic pH values. The results of this research have demonstrated that even minimal acid exposure (around 1 hour in duration) can enhance the strength of gellan fluid gels, to the point of solidification, as it seems to reinforce the preexisting cross-linked biopolymer structure and has previously been confirmed in similar antecedent studies. Additionally, comparable observations have been made for alginate gels and consequently, may indicate the suitability of these polysaccharides for inclusion in the treatment of osteochondral or osseous tissue defects,

which, as previously mentioned, can be associated with a reduced pH due to local inflammation [17, 66, 67, 68, 69].

Biochemistry/Cell viability

As previously mentioned, alginate hydrogels have been successfully employed in the encapsulation of fibroblast cells, with demonstrated cell viability over 60 days, irrespective of gel concentration [51]. Moreover, viability was maintained for a further 90 days, which may be attributed to the vastly hydrated morphology of hydrogels, comparable in structure to the extracellular matrix (ECM), that can facilitate perfusion of nutrients and waste products, as well as support paracrine signalling [70, 71, 72]. However, the metabolic activity and proliferation of these cells was found to be suppressed by the mechanically confining architecture of the hydrogel and subsequent work has also elicited the lack of ECM deposition by cells encapsulated in hydrogel substrates, which is essential for tissue regeneration [72, 73]. Therefore, this prompts consideration of cells that are responsive to their physical and chemical environment, such as mesenchymal stem cells, whose differentiation pathways can be significantly influenced by factors such as the porosity and stiffness of the matrix. In particular, they are extremely sensitive to the elastic properties of the material, which suggests that encapsulation of these cells within hydrophilic gels may result in their inadvertent differentiation due to imposition of external forces [74]. Alternatively, investigations have been made into the use of fluid gel scaffolds for cellular delivery, which enable the suspension of cells between the interstices within the liquid component of the fluid gel system, without changing the basic composition of the gel. Additionally, Paxton et al. have established excellent cell viability of MC-3T3 cells within 1% agarose fluid gels over a 24 h period, although agarose itself may be unsuitable for tissue regeneration applications owing to its non-degradable qualities [70, 75].

Temperature response

In consideration of therapeutic applications for gels, a significant factor that could affect their stability *in vivo* is the physiological temperature of the body. Though this would not occur in

isolation, but in conjunction with the impact of shear force, which together can deteriorate the mechanical properties of the gel. As illustrated in Figure 2.5, the yield stress of the gel can shift as a function of temperature, which, for alginate fluid gels, indicates a decrease in its initial viscosity at 37°C [36].

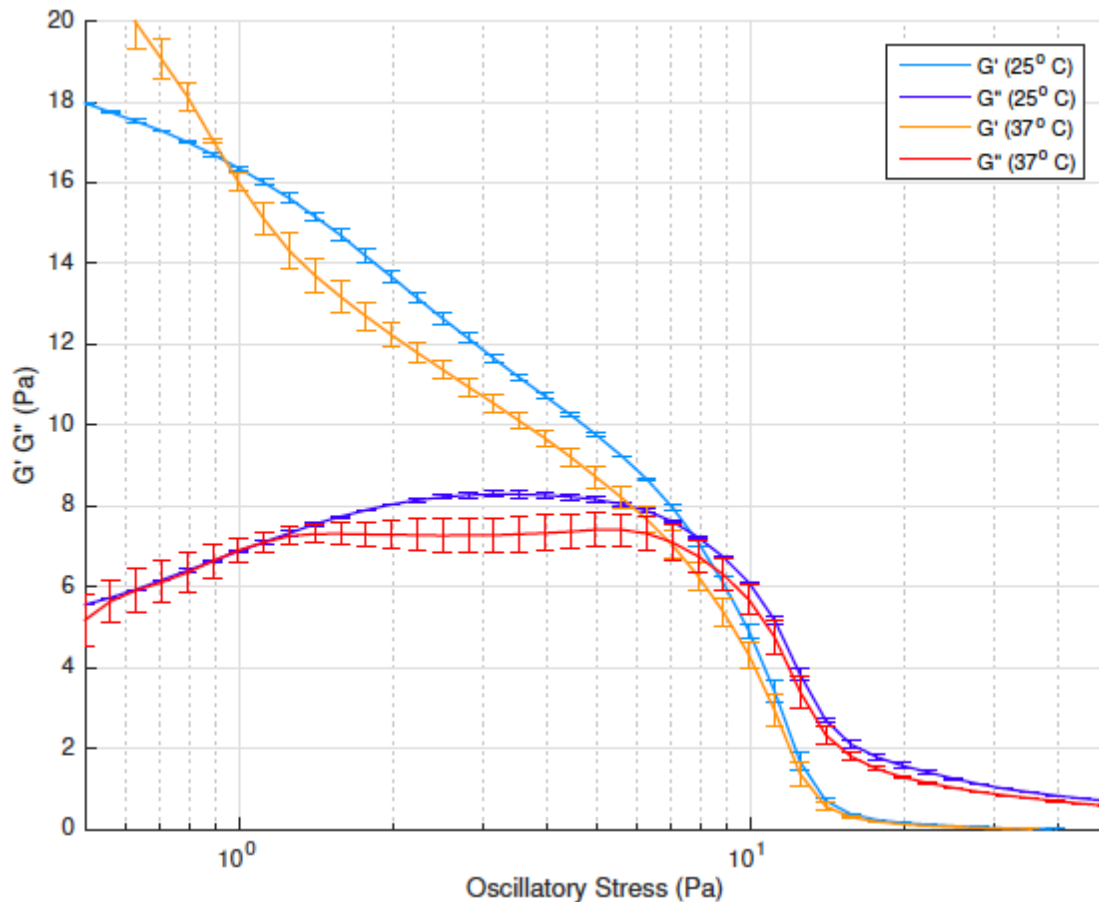


Figure 2.5: The variation between the storage (G') and loss (G'') moduli of 1% alginate fluid gels at 25°C and 37°C, formulated with 0.1M CaCl_2 [36].

These effects may also have implications for gel sterilisation procedures, as processes such as autoclaving can utilise temperatures in excess of 120°C, causing decomposition of the gel structure. For sodium alginate gels (1% and 3%) crosslinked with 0.1M CaCl_2 , this is a result of depolymerisation and is more discernible in gels of greater molecular weight or higher polymer concentration. This is believed to be synonymous across other biopolymer materials and may be seen as a consequence of entropic dominance, forcing the expulsion of water from the gel and hence, collapse of its supportive infrastructure [61, 76, 77]. However, reduction of the

sterilisation temperature has been correlated with a lower deficit in gel stability[78, 76, 77]. Furthermore, it is possible to minimise the degree of depolymerisation through autoclaving by increasing the pH value of the alginate solution to pH 7.0-8.0. [45, 79]. Alternatively, steam sterilisation has been established as a more feasible substitute, particularly for gellan gel products designed for ocular administration, whose strength is considerably diminished following autoclaving [80].

CHAPTER 3

BONE MARROW ASPIRATE CONCENTRATE (BMAC): EXISTING AND POTENTIAL METHODS OF DELIVERY

3.1 Bone Marrow Aspirate Concentrate (BMAC)

Bone Marrow Aspirate Concentrate (BMAC) consists of a heterogeneous population of cells, predominantly neutrophils and erythroblasts, but also includes lymphocytes, eosinophils, monocytes and basophils. Of the mono-nucleated cells, bone marrow-derived MSCs (BM-MSCs) account for a mere 0.001 to 0.1%, with the remaining volume of BMAC being made up of a vast number of platelets, growth factors and cytokines, which are inter-related [81, 82, 83, 84, 85]. Currently, there is steadily growing interest in the application of BMAC for cartilage repair and regeneration, owing to promising results obtained in small and large animal models, as well as initial human trials [81, 86]. This has included evidence of hyaline like cartilage production, without any reported adverse events or harvest site morbidity [81]. However, additional interest has been expressed in platelet-rich plasma (PRP), which has also indicated positive treatment outcomes in cartilage defect repair, including enhanced joint function [81, 87]. Through the centrifugation of peripheral blood, PRP is associated with a supraphysiological number of platelets that contain a large concentration and variety of growth factors. Consequently, these can help stimulate local angiogenesis and modulate the inflammatory effects of tissue damage, amongst numerous other functions [87, 88]. Owing to their similarity in composition, BMAC has actually been described as PRP with the exception of an additional stem cell population [87]. Although, after analysing the cellular composition and cytokine concentrations of both

BMAC and PRP, it was found that BMAC encompassed approximately 2.5 times the platelet concentration of PRP, as well as almost 12 and 20 times the number of white blood cells and neutrophils, respectively. Potentially resulting from this higher concentration of platelets, the average concentration of growth factors and cytokines, such as vascular endothelial growth factor (VEGF), interleukin-8 (IL-8) and transforming growth factor- β 2 (TGF- β 2), was markedly greater in BMAC than PRP, as these reside within the alpha granules of platelets [81, 87].

Considering this composition in further detail, it is clear that the positive clinical findings of utilising BMAC in the treatment of cartilage defects are supported by the underpinning biological actions of some of these growth factors. In particular, IL-8 has been found to encourage migration of BM-derived cells, such as MSCs, to the defect site and also augment VEGF production, thus improving angiogenesis that is essential for epiphyseal vascular supply and cartilage regeneration [81, 89]. Perhaps more prominently recognised is the TGF superfamily that comprises TGF- β 1, TGF- β 2, TGF- β 3, along with BMP-2 and BMP-7. All of which are required in a cascade of pathways that ultimately lead to chondrogenesis and chondrocyte expansion [81, 90]. Specifically, TGF- β 2 has shown greater efficacy in promoting chondrogenesis than TGF- β 1, though it acts synergistically with BMP-2 to stimulate chondrogenic differentiation of MSCs *in vitro* [81, 91]. BMP-7 also has an important role to play in cartilage tissue formation, as it can enhance extracellular matrix production and seems unique in its ability to remain unaffected by common debilitating factors, such as age [81, 90]. Other mentionable growth factors that are likely contributing to its success in human and animal models include insulin-like growth factor (IGF-1) and the family of fibroblast growth factors (FGF), which are associated with elevated collagen and proteoglycan synthesis and improved BMP signalling, leading to greater and earlier differentiation of MSCs, respectively [81, 92, 93, 94, 95, 96].

BMAC is primarily obtained through aspiration of bone marrow from the iliac crest, as this has been reported to contain, on average, higher concentrations of MSCs [83]. Although, it is still uncertain as to the clinically effective quantity of MSCs that would be required for cartilage

repair [87]. Following aspiration, the BMAC is then heparinised and filtered, before being concentrated through the use of a commercially available system, typically the Harvest BMAC[®] SmartPrep2[®], which has been shown to be superior in isolating greater numbers of progenitor cells [97, 98].

3.2 Existing and potential methods of delivery

The ability to collect the aspirate and combine it with a delivery matrix at the patient bedside, potentially circumvents the need of having to extract a cell population and expand them off-site before reintroducing them into the patient at a later date. There are currently a number of existing scaffolds that could and have been used to support the structure of BMAC and in some cases, form a clot to stabilise and enable its delivery in the form of an implant. The most promising of which is a chitosan-based product, known as BST-CarGel[®], which was designed to be combined with a patient's whole blood before being injected into their cartilage defect. BST-CarGel[®] is successful in that it is capable of producing a physically stable and injectable implant, with demonstrated cell viability of BMAC until natural clot degradation, thus proving its suitability as a one-stage cell based treatment [97, 99, 100]. However, its efficacy and application with BMAC has yet to be established in *in vivo* studies and it is not appropriate for all defects [99, 100, 101].

Other potential scaffolds that are commercially available include Chondro-Gide and Alpha Chondro Shield. Chondro-Gide is formed of naturally occurring type I and type III collagen, arranged in a bilayered structure, featuring both a porous surface and a compact surface that enables cell adhesion and inhibits cell effluence, respectively. This creates a strong and resilient scaffold that has received extensive clinical application in autologous matrix induced chondrogenesis (AMIC) operations and autologous chondrocyte implantation (ACI), however it does require fixation within defects using either suturing or fibrin glue [102, 103, 104, 105, 106]. In contrast, Alpha Chondro Shield comprises a synthetic, non-woven homogeneous network

of polyglycolic acid (PGA) fibres, which was designed for use with microfracture treatments for simple, practical and off-the-shelf application. Although, to date, there has been no clinical evidence published regarding its use with MSCs or chondrocytes and furthermore, *in vitro* data comparing chondrogenic differentiation and culture of BM-MSCs and adipose tissue-derived MSCs (AT-MSCs), indicates that the fast degrading PGA fibres in Alpha Chondro Shield fail to support cell growth and proliferation. Additionally, it has been suggested that PGA based biomaterials may be susceptible to release acidic degradation products throughout long term culture, which would clearly impede cell proliferation [102, 103].

In work by Kohli et al., Chondro Gide and Alpha Chondro Shield were examined along with with a third clinical grade scaffold, Hyalofast™, which is composed of a non-woven, naturally occurring hyaluronic acid-based membrane, for the original purpose of treating chondral and osteochondral defects by ensnaring MSCs *in situ*. This scaffold has demonstrated both adherent and malleable properties, when combined with BMAC for clinical repair, as well as promising results after 2 years follow up. However, following *in vitro* analysis, it was revealed that its structure deteriorated in long term culture and poor cell retention was observed. Though, this highlights a clear barrier between bench-to-bedside translation, since *in vitro* studies can not effectively mimic the conditions and environment that exist *in vivo* [102, 103, 107]. Similarly, another hyaluronic acid-based scaffold, Hyalograft C® has contributed to the production of primarily hyaline-like cartilage repair tissue in recent clinical trials, when used in conjunction with autologous chondrocyte implantation. Its structure is also fabricated from a matrix of 20- μ m-thick fibres, creating a porous network with varying sized interstices. Although, in 2013, the European Medical Association (EMA) made the decision to remove Hyalograft C from the European market, after reporting concerns surrounding their manufacturing processes and the standard of evidence that they presented for approval [102, 108, 106, 109].

One can therefore infer some common features and characteristics that are essential for an optimum delivery vehicle that will sustain a population of cells and provide the correct biochemical

microenvironment to direct their lineage down a chondrogenic or osteogenic route. From the aforementioned case studies that have been discussed, it seems beneficial to utilise natural materials that have good biocompatibility, with particular preference being given to collagen and hyaluronic acid, as a consequence of their native presence in cartilage tissue [102]. Ideally, the scaffold would also be biodegradable at a rate that will enable simultaneous regeneration of the tissue, possibly through facilitating extracellular matrix production by autologous cells, whilst avoiding generation of concentrated acids or debris that could cause local inflammation and apoptosis [102, 106, 101]. As a result, the structure of the implant would need to have suitable porosity to allow migration of cells, growth factors and cytokines *in vivo*, but would additionally require appropriate stiffness and mechanical properties, as this influences MSC differentiation [102, 110]. Furthermore, this property would determine its ability to maintain stability *in situ*, particularly if the delivery vehicle possesses fluidity upon application, which would be desirable to accommodate injectable treatment with the scaffold. By formulating such a implant, one can also satisfy fitting a variety of shapes and forms associated with cartilage defects, as the architecture would be able to conform to the nature of the defect. Evidently, a tissue-adhesive quality may be favourable, as it was previously mentioned that many scaffolds require the use of sutures or biological or synthetic glues in order to ensure that they are retained in the defect. BST-Cargel is unique, however, in that it possesses this characteristic as a result of its polycationic nature [102, 101, 99]. Another advantage of BST-Cargel is its physiological pH compatibility, as well as its excellent viscosity profile that enables it to mix homogeneously with whole blood or BMAC and subsequently form a stabilised blood clot within a 15 minute clotting timeframe. This therefore permits an ideal, minimally invasive, single step administration of the scaffold for cartilage repair [101, 99, 97].

Finally, a delivery vehicle that is reproducible, economical and can support differentiation and integration of cells *in vivo*, is evidently the ultimate ambition for scaffold design [83, 106].

CHAPTER 4

RESULTS CHAPTER 1: FORMULATION OF SHEAR-THINNING GEL SYSTEM AND CELL VIABILITY WITHIN FLUID GELS

As previously discussed (Chapters 1, 2 and 3), a suitable delivery matrix would possess fluidity upon application in order to accommodate parenteral administration and would ideally 'set' *in situ* upon removal of shear forces, without the use of any additional chemical agents. Furthermore, the significance of maintaining cell viability was also considered, leading to the conduct of the following experiments.

4.1 Materials and Methods

4.1.1 Materials

The following materials were purchased from Sigma-Aldrich: Anhydrous calcium chloride (CaCl_2 , 110.98g/mol, C1016), $\geq 93\%$, granular $\leq 7\text{mm}$; Alginic acid sodium salt ($\text{NaC}_6\text{H}_7\text{O}_6$) powder (180947) and medium viscosity from brown algae (A2033) and Dulbecco's phosphate buffered saline (PBS) (D8537). DI H_2O was obtained from Biochemical Engineering laboratory G13.

Preparation of sample materials

A 500ml 1M calcium chloride solution was prepared by dissolving 55.49g of CaCl_2 in DI H_2O . This was then used to obtain a diluted 100ml 0.1M calcium chloride solution. For production of alginate fluid gels, 1% and 2% alginate solutions were made using a magnetic hot plate stirrer

(set to 400rpm) to dissolve 1g and 2g, respectively, of alginic acid sodium salt in 100ml of DI H₂O (heated to 60°C) over a 2 hour period. A Kern (Germany) 440-35N mass balance and Ohaus Pioneer PA114 analytical balance were used to weigh out all sample materials.

Formulation of alginate fluid gels

Formulation of fluid gels and shear testing were carried out using a TA Instruments AR-G2 Rheometer (9B4032), with a temperature-controlled concentric cylinder (4000 μ m gap) and 14mm four-blade vaned rotor geometry (993058). The system was self-calibrated through rotational mapping of the connected geometry and between experiments, the cylinder and vaned rotor were detached and cleaned using DI H₂O. This was operated with a compressed air supply (40psi) and Julabo water bath (FP35), in conjunction with Rheology Advantage Instrument Control AR and Rheology Advantage Data Analysis software. A procedure file was created with the following specification:

- Test type: *Temperature ramp*
- From: *60°C to 30°C*
- Wait for start temperature: ☒
- Ramp rate: *1.5°C min⁻¹*
- Sample points: *20*
- Controlled variable: *Shear rate: 450 s⁻¹*

Additionally, fluid gels were produced using a Peak hold ramp, with the following specification:

- Step name: *Conditioning step*
- Initial temperature: *20.0°C*
- Wait for correct temperature: *Yes*
- Do set temperature: *Yes*
- Wait for normal force: *No*
- Perform pre-shear: *No*
- Perform equilibration *Yes*

- Equilibration duration: *0:01:00 (hh:mm:ss)*
- Wait for zero velocity: *No*
- Control normal force: *Uses current instrument settings*
- Purge gas only: *No*

- Step name: *Peak hold step*
- Test type: *Peak hold ramp*
- Controlled variable: *Shear rate: 500 s⁻¹*
- Duration: *0:30:00 (hh:mm:ss)*
- Delay time: *0:00:00 (hh:mm:ss)*
- Temperature: *20.0°C*
- Wait for start temperature: *No*
- Motor mode: *auto*

Initially, 18ml volumes ($\pm 0.02\text{ml}$) of 1% alginate solution were added into the concentric cylinder by pipette, followed by 2ml ($\pm 0.02\text{ml}$) volumes of 0.1M CaCl_2 solution, heated to 60°C ($\pm 1.0^\circ\text{C}$). The CaCl_2 solution was added manually in a dropwise manner the righthand side of the cylinder, as soon as the temperature ramp was initiated at 60°C . Subsequently, 27ml ($\pm 0.03\text{ml}$) and 3ml ($\pm 0.03\text{ml}$) volumes of 2% alginate and 0.1M CaCl_2 solution were used, respectively.

Rheological testing - Strain and frequency sweeps

Since fluid gels exhibit viscoelastic behaviour, they can be described in terms of their viscous and elastic components; their storage modulus (G') and loss modulus (G''), respectively, since the elastic response of the material represents the energy stored during the deformation process and the viscous response represents the energy lost through heat during deformation. Consequently, materials with a higher G' than G'' exhibit more solid like behaviour and those with a greater G'' than G' behave more as a liquid [111, 112]. These viscoelastic properties can ei-

ther be established using dynamic or transient testing, however the latter, which includes stress relaxation and creep testing, is limited by the fact that the behaviour of the material cannot be described in terms of the frequency. Therefore, for the purpose of this study dynamic testing was used to obtain all rheological measurements. These types of test involve the application of a small sinusoidal strain (γ) (or stress (σ)), whilst simultaneously measuring the stress (or strain) produced in the material [111]. This can conveniently be described by the following equation:

$$\sigma(t) = \gamma_0 G'(\omega) \sin(\omega t) + \gamma_0 G''(\omega) \cos(\omega t) \quad (4.1)$$

where G' and G'' are both functions of the angular frequency, ω [111].

Following formulation, rheological tests were performed on fluid gels using an ARG2 Rheometer (TA Instruments) with two 40mm stainless steel sandblasted parallel plates (AC20-3 Cover Plate and 993244, TA Instruments) in order to prevent slippage. Strain sweeps were performed to determine the Linear Viscoelastic Region (LVR) of the fluid gels, in which the stress is independent of the strain [112]. Accordingly, an oscillation procedure file was created, using a constant frequency of 1.0 Hz, at 37°C, in a strain range of 0.1 - 500%. Frequency sweeps were also performed as part of the oscillation procedure, using a frequency range of 0.1 - 100.0 Hz, at 37°C, at a fixed strain of 0.5%.

4.1.2 Cell culture

MC3T3 fibroblasts were obtained from the American Type Culture Collection (ATCC) and cultured in high-glucose Dulbecco's modified Eagle's medium (DMEM) supplemented with 10% Fetal Bovine Serum (FBS) (Sigma-Aldrich F7524, UK) and 1%vol Penicillin/Streptomycin (P4333-100ml Sigma-Aldrich, UK). The culture medium was exchanged every two or three days and cells were incubated in a 5% CO₂ incubator at 37°C.

4.1.3 Fibroblast suspension within alginate fluid gels

1% and 2% w/v medium viscosity sodium alginate fluid gels, produced as described in 4.1, were exposed to UV-irradiation within a sterile biosafety cabinet, with laminar flow, for a minimum of 30 minutes, prior to suspension of MC3T3 fibroblasts and culture within Petri dishes.

4.1.4 Live/dead staining

Cell viability was analysed qualitatively using calcein AM and propidium iodide staining. Images of stained cells were then captured using confocal laser scanning microscopy (Olympus FV1000, Multiple Ar laser, Germany).

4.2 Results and discussion

4.2.1 Characterising fluid gels in terms of their rheological profile

Fluid gels were characterised in terms of their rheological profile, using methods outlined in 4.1.1. This measured the storage modulus (G'), loss modulus (G'') and complex viscosity (η^*) of 2% alginate fluid gels at 37°C, in order to simulate their mechanical behaviour *in vivo*. After conducting strain sweep testing, the LVR was determined as below 10% strain. Therefore, frequency sweep testing was performed in this range, at 0.5% strain, which was consistent with previous studies [32, 113, 114].

Previous work had been conducted on 2% alginate fluid gels formulated using a temperature ramp from 60°- 30°C, however an original study conducted by Streather described the production of alginate fluid gels using a slightly more extensive temperature ramp, from 60°- 25°C [37, 36]. Therefore, 2% alginate fluid gels using three different formulation procedures were produced and analysed by examining the frequency dependence of G' and G'' in the LVR.

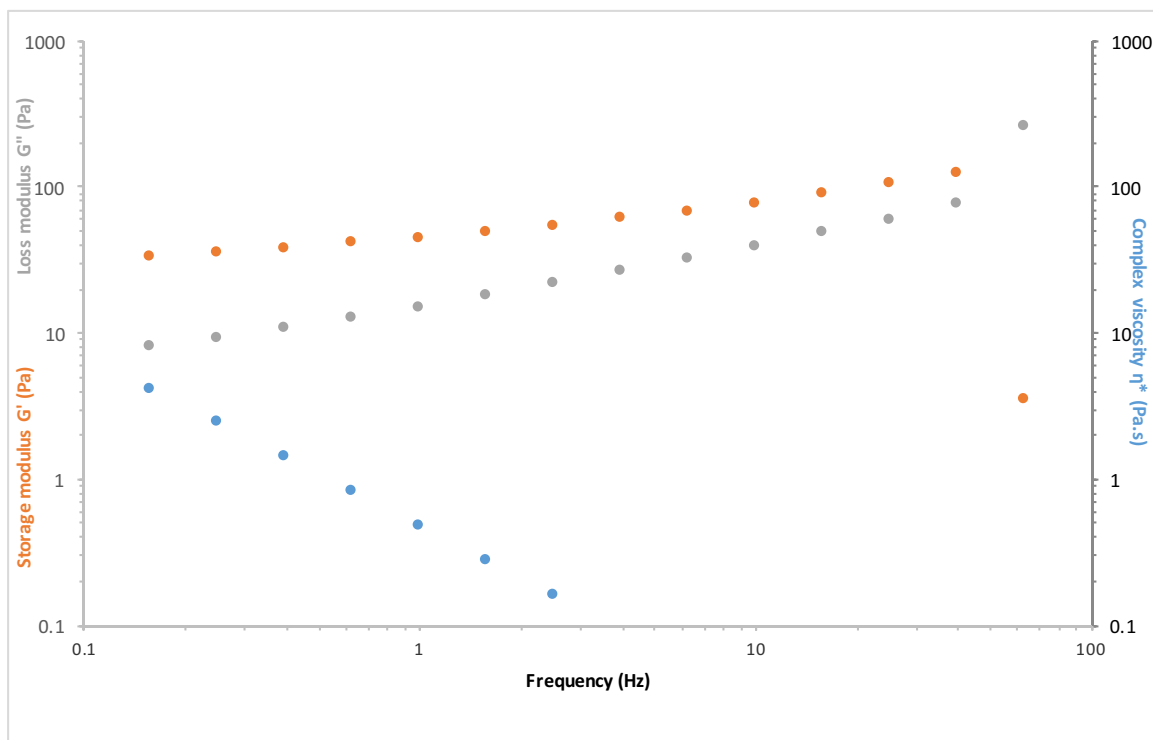
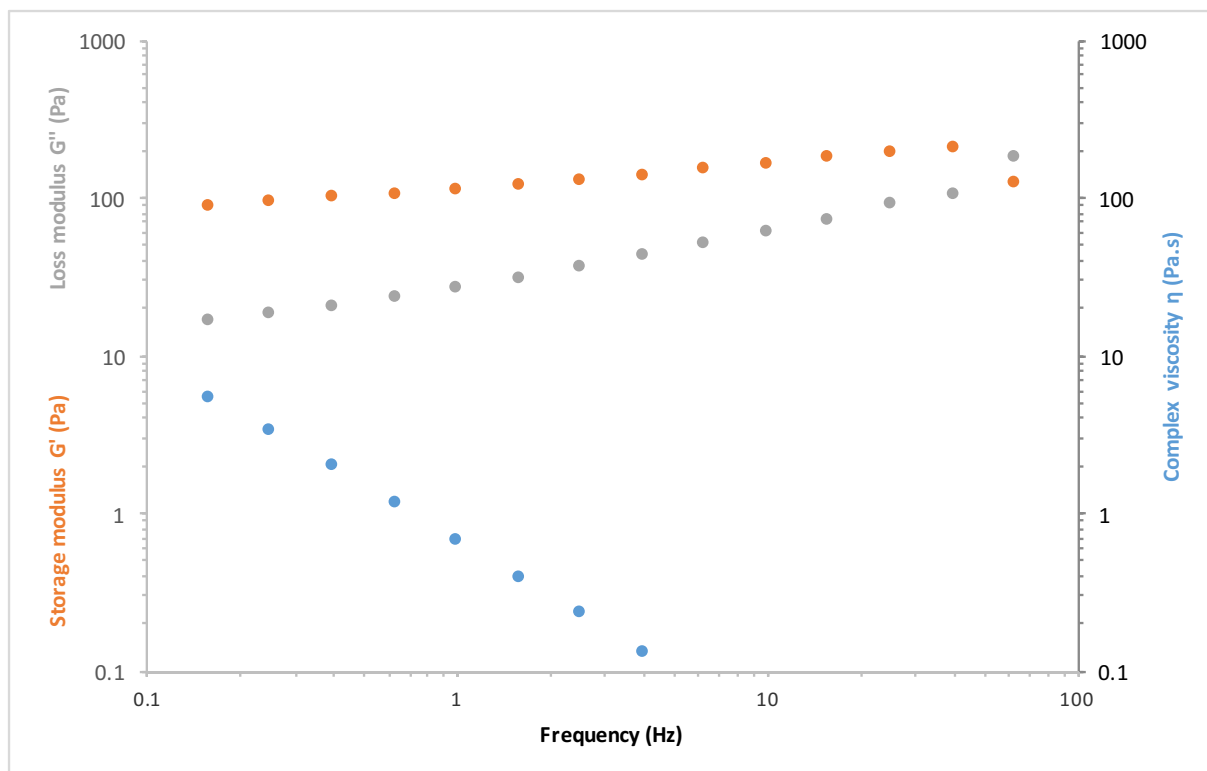


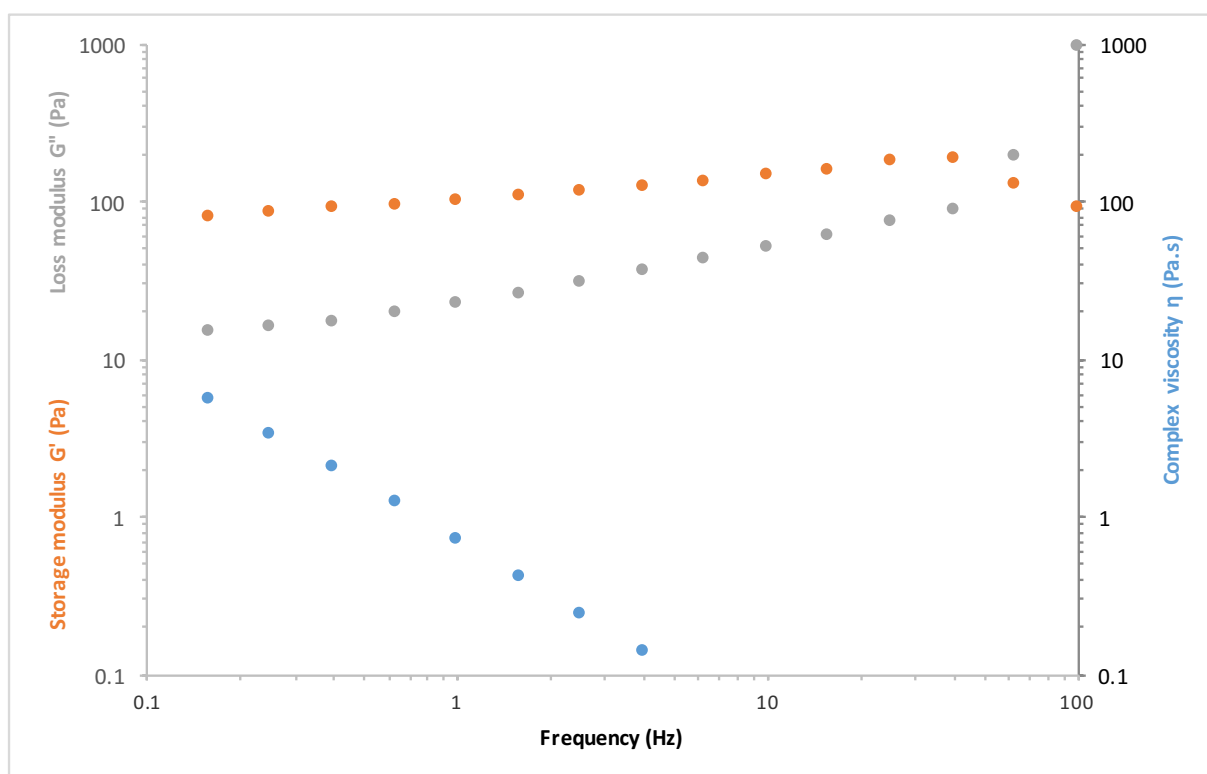
Figure 4.1: The variation between the storage (G') and loss (G'') moduli and the resulting complex viscosity of 2% alginate fluid gels at 37°C, formulated with 0.1M CaCl_2 using a temperature ramp from 60°- 25°C.

For 2% alginate fluid gels formulated using a temperature ramp from 60°- 25°C, the dominance of the storage modulus (G') over the loss modulus (G'') was seen for up to a frequency of almost 65 Hz, when the fluid gel would behave more as a liquid and is confirmed by the decrease in the complex viscosity (η^*) (Fig. 4.1). Up to this frequency, the storage modulus was recorded as approximately 120 Pa, which was slightly higher than what had been measured previously for 2% alginate fluid gels that were produced using a pin stirrer method [115].

A similar profile was seen for 2% alginate fluid gels formulated with a temperature ramp from 60°- 30°C ,(Fig. 4.2), after 24 hours post-formulation. However, up to the frequency of approximately 65 Hz, the storage modulus was measured at around 202 Pa, remarkably higher than was recorded for the 60°- 25°C formulation. Although, this measurement was then repeated following a further 24 hours and it was found to have to reduced by almost 10% to 185 Pa, highlighting the importance of conducting degradation studies on these type of gels.

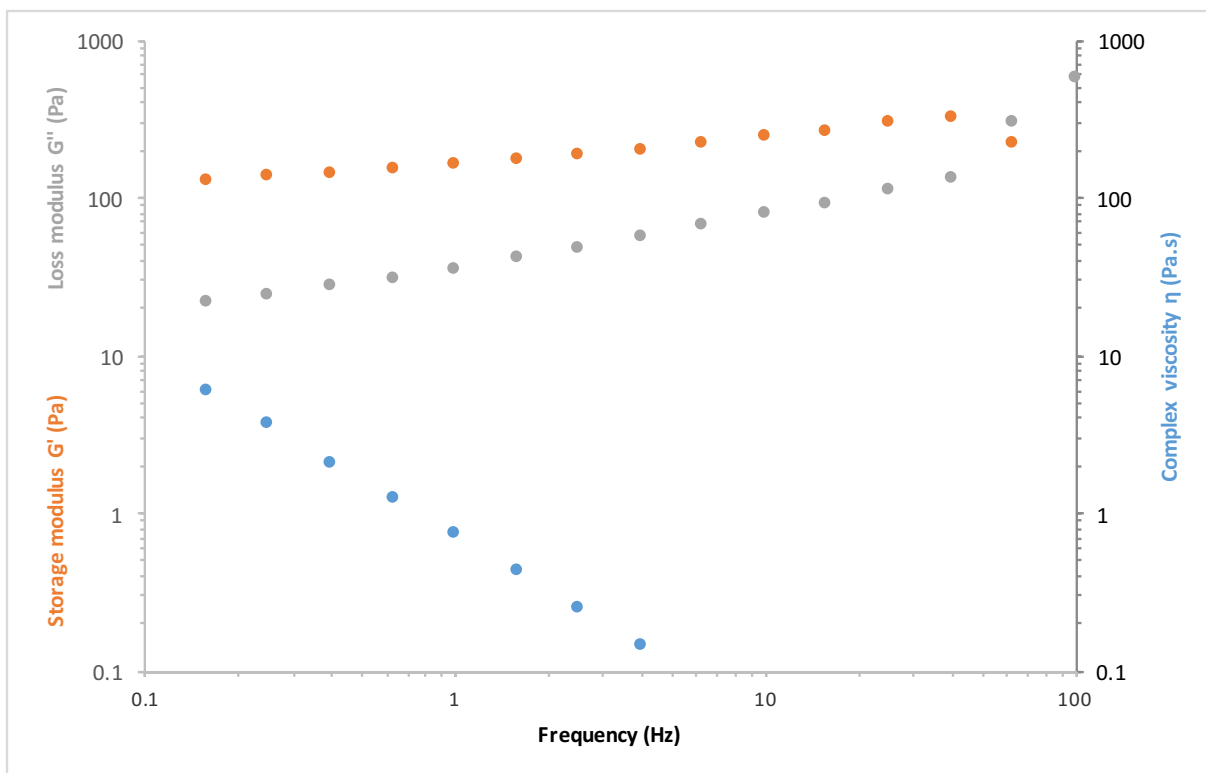


(a) 24 hours post-formulation

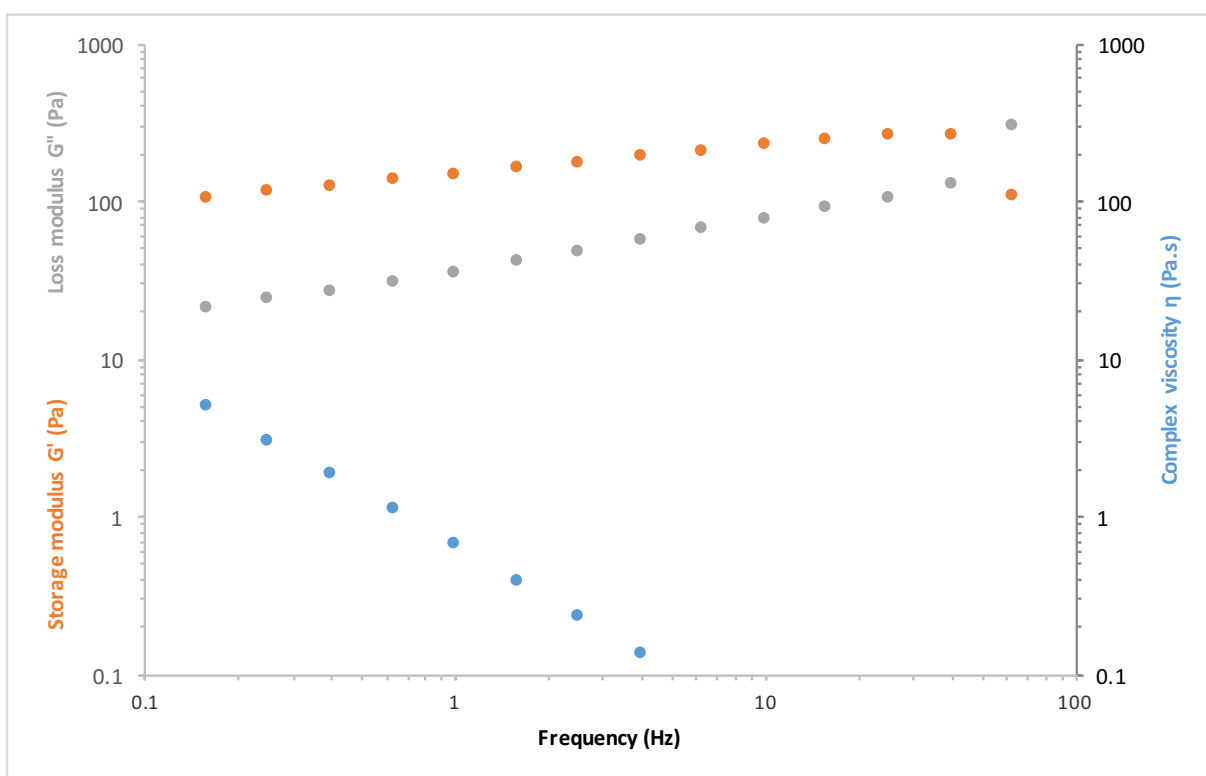


(b) 48 hours post-formulation

Figure 4.2: The variation between the storage (G') and loss (G'') moduli and the resulting complex viscosity of 2% alginate fluid gels at 37°C, (a) 24 hours post-formulation with 0.1M CaCl_2 (b) 48 hours post-formulation, using a temperature ramp from 60°- 30°C.



(a) 24 hours post-formulation



(b) 48 hours post-formulation

Figure 4.3: The variation between the storage (G') and loss (G'') moduli and the resulting complex viscosity of 2% alginate fluid gels at 37°C, (a) 24 hours post-formulation with 0.1M CaCl_2 (b) 48 hours post-formulation, using a peak hold ramp at 20°C and a constant shear rate of 500 s^{-1} .

This was also the case for 2% alginate fluid gels produced using a isothermal peak hold ramp at 500s^{-1} . As illustrated in Figure 4.3, there was a 20% reduction in the storage modulus at the same frequency of approximately 65 Hz, after 48 hours post-formulation. Though, the peak hold procedure used may be preferential over the temperature ramp profiles, since the storage modulus recorded up to this frequency was much greater, at 324 Pa.

In the case of all three formulations for alginate fluid gels, the frequency sweep analysis characterised uniform gel-like behaviour across the frequency range considered, correlating with previous work [115]. This has formerly been described on a scale between a ‘weak gel’ and a ‘strong gel’ with regards to the relationship between the frequency and G' and G'' . The nature of the ‘elastic’ and ‘hairy’, ‘strong gel’ particulates; enabling the formation of a loose network and structure within the fluid gel, combined with the ‘weak gel’ configuration; permitting the flow of this network under shear, is what distinguishes the fluid gel microstructure from other types of gel [32, 115]. For each of the formulations discussed, there were seemingly gradual increases in the elastic component of the fluid gels, in terms of their storage modulus, G' , up to the point where the viscous element, measured by G'' , began to dominate. This further illustrates the resistance of polymer structure to an applied force, quintessential to that of an elastic material.

4.2.2 Tailoring formulation processing parameters for different applications

As previously shown in 2.2.1, from Figure 2.3, it is clear that the resting properties of fluid gels can also be modulated by adjusting the cooling rate of the formulation, as this affects the initial viscosity of the system under essentially zero shear force. This would allow very fine control over the resting viscosity for low viscosity ranges from approximately 4 - 13 Pa.s. In order to increase the initial viscosity, the weight percentage of the polymer must be increased. This has been established by the data given in Figure 4.4, which demonstrates that by increasing the weight percentage of the polymer by 1% to 2%, whilst observing the same cooling rate, a

fluid gel with an initial viscosity of around 37 Pa.s can be fabricated that is quite strongly shape maintaining and therefore, relatively stiff in nature. The significance of this work highlights the different applications that would be suitable for each type of gel, based on its resting properties. For example, a 1% fluid gel, with a lower initial viscosity, could be useful for topical application, potentially as a skin cream that would permit spreading, but would not necessarily require mechanical stiffness or a high resting viscosity, as it would not need to endure significant pressure. However, it might be less appropriate to utilise this gel in orthopaedic applications, in load bearing joints, as the gel may be susceptible to seepage from the defect, or in an articulating joint, it could be subject to a constant degree of shear from the joint space, which may prevent the gel from regaining its initial viscosity. In this case, a fluid gel with a higher resting viscosity would be more applicable, which would be capable of tolerating higher rates of shear force.

Consistent with earlier work that has explored the mechanical spectra of alginate fluid gels as a function of polymer concentration, the 2% alginate fluid gel system exhibited a greater shear-viscosity profile under shear compared to the 1% fluid gel system, as illustrated in Figure 4.4 [115]. Although, whilst both formulations demonstrated injectable properties, the increased viscosity of the 2% gel system showed greater retention within model defects and improved self-setting ability (Fig. 4.5). This would be more significant in clinical practice, where minimal operative time would be preferred and would also reduce the likelihood of infection at the defect site.

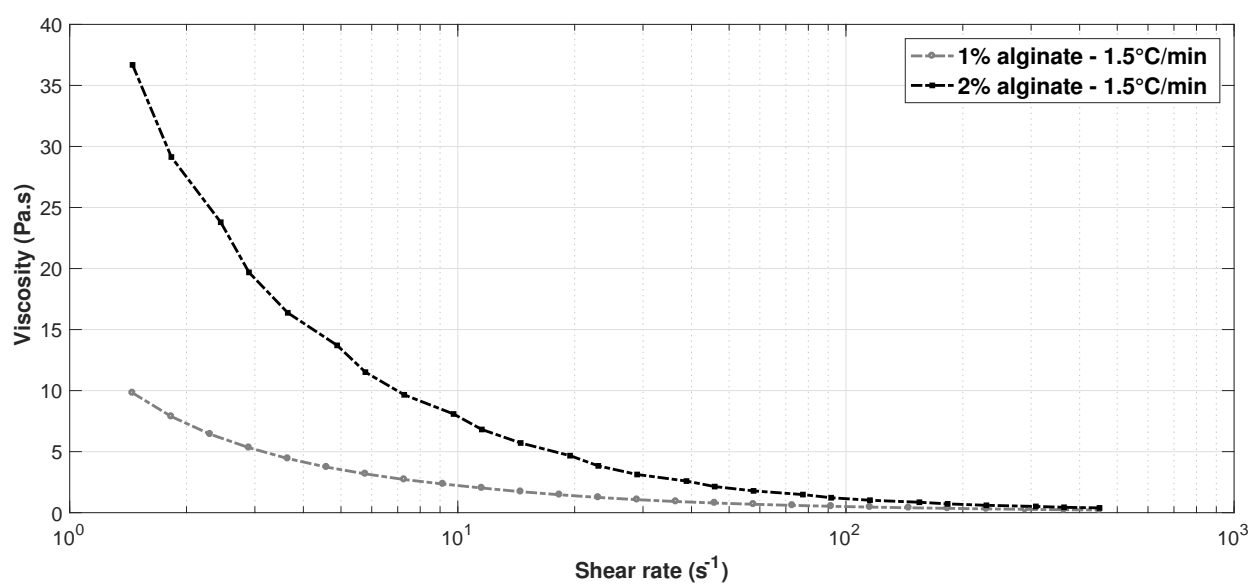


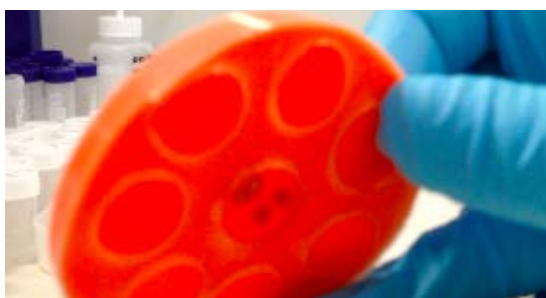
Figure 4.4: The rheological profile difference between 1% and 2% alginate fluid gels, with an initial production volume of 30ml and 0.1M $CaCl_2$ addition, formulated at 1.5°C cooling rate.



(a) Injectable application



(b) Post application



(c) Pre-inversion



(d) Mid-inversion



(e) Mid-inversion



(f) Post-inversion

Figure 4.5: Still frames demonstrating injectable application of 2% alginate fluid gel and bead system into model cartilage defect, with alginate beads dyed red for clarity.

4.2.3 Visualisation of the fluid gel structure

As an acidic polysaccharide, fluid gels manufactured using sodium alginate acid are susceptible to staining by the cationic dye Alcian blue, through what is thought to be the establishment

of salt linkages with the acidic groups of anionic polymers [116]. This has been illustrated in Figures 4.6 and 4.7 that reveal an alignment of strands or fibres in the fluid gel microstructure, which may contribute to its mechanical properties, which were originally thought to result from the network of fluid gel particulates formed through conformational ordering of hydrocolloid chains [37]. These optical micrographs of 2% alginate fluid gels are substantially clearer and enable more discerning features to be elicited than images previously taken for 3% alginate and 2% kappa-carrageenan fluid gels, following their dilution with deionised water [38, 115]. Similar findings have recently been discovered with fluid gels manufactured using gellan gum, therefore future work will include further characterisation of the fluid gel microstructure, through both phase contrast and confocal microscopy by fluorescently labelling the alginate biopolymer.



Figure 4.6: Alcian blue staining of 2% medium viscosity alginate fluid gels, formulated using (A) 60-25°C and (C) 60-30°C temperature profiles, for identification and visualisation of their microstructure on (B) glass slides.

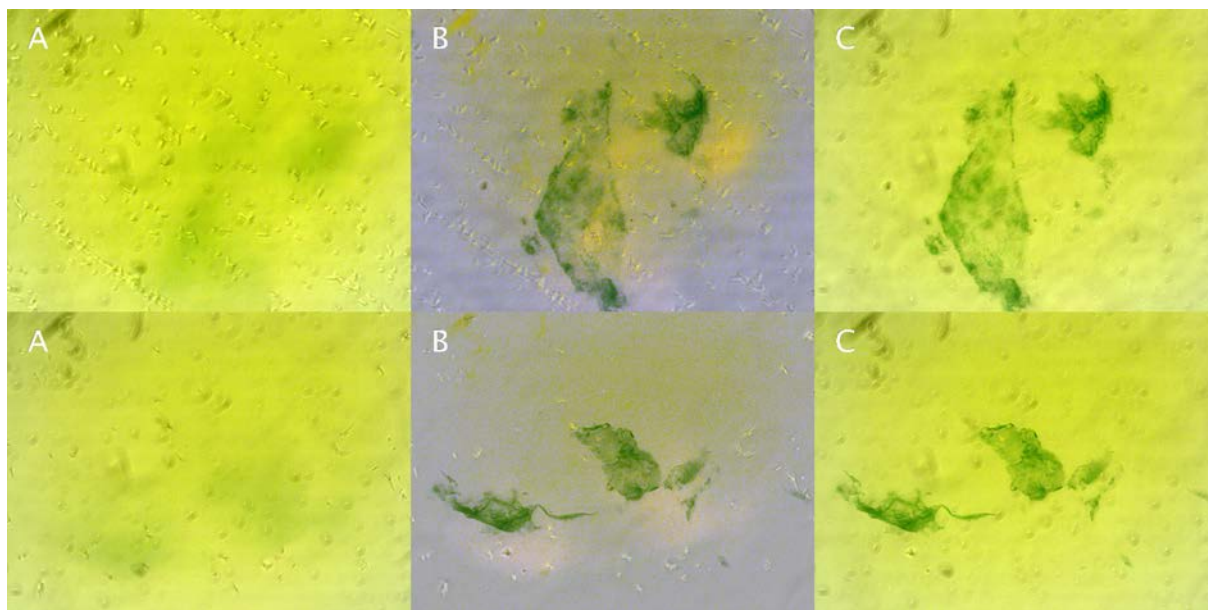


Figure 4.7: Brightfield images illustrating microstructure of 2% medium viscosity alginate fluid gels stained with alcian blue and imaged on two different focal planes ((A) and (C)), overlapping in (B) (magnification x10).

4.2.4 Live/dead staining of MC3T3 fibroblasts within alginate fluid gels

Following formulation and characterisation of the fluid gel microstructure, recent efforts were made to evaluate the viability of a MC3T3 fibroblast cell population within 1% and 2% alginate fluid gels. Initial results have provided promising evidence, with a large proportion of the population expressing excellent viability after 7 days in culture and no significant fibroblast death was observed (Fig. 4.8).

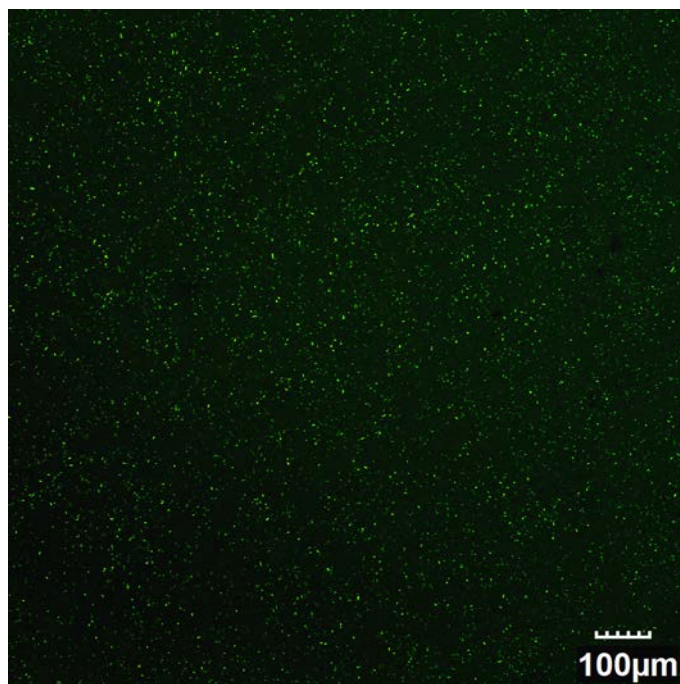


Figure 4.8: Calcein-AM/PI live/dead staining of MC3T3 fibroblasts in 2% w/v alginate fluid gel, cross-linked with 0.1M CaCl_2 , after 7 days. Live and dead cells stain green and red, respectively, with the majority of cells remaining viable following 7 days of culture within the fluid gel matrix and no significant fibroblast death observed.

4.2.5 Live/dead staining of BMAC cells

Further work has now been conducted with human BMAC, which was combined with the fluid gel material within quadrant Petri dishes. This was subsequently visualised using Calcein-AM/PI live/dead staining to assess the viability and distribution of cells within the matrix, which can be seen in Figure 4.9. Overall, the cells seem to express good viability following incorporation with the gel scaffold, though some apoptotic cells can be observed, but would be anticipated for primary human cell culture, as they are generally more fragile and sensitive to their environment. It was therefore necessary to attempt to sterilise the fluid gel material prior to combination with the BMAC, as it is currently not manufactured under sterile conditions. Consequently, for this preliminary work, small volumes of the gel were placed in shallow petri dishes and exposed to UV-irradiation within a sterile biosafety cabinet, with laminar flow, for a minimum of 30 minutes. However, whilst this sterilisation procedure is beneficial for preserv-

ing the mechanical properties of the gel, it cannot sufficiently eliminate the presence of bacteria in alginate gel samples that have previously been contaminated with *E. coli*, as it is largely dependent on the thickness of the material and its ability to absorb the specific wavelength of the light. Thus, this can help explain the ultimate infection of the BMAC samples incorporated into the alginate fluid gel scaffolds, but the limitation of the study was that UV irradiation was only administered for 20 minutes on each side of the gel, so it is possible that prolonged UV exposure, such as 48 hours, may be more effective for terminal sterilisation of the gel. Other potential terminal sterilisation methods that have been explored for alginate gels include autoclaving and gamma-irradiation, which can both guarantee complete removal of bacterial species, although they compromise the mechanical integrity of the gel structures and result in degradation of polymer fibres. Ethylene oxide gas treatment has also been considered for terminal sterilisation, but as a potentially toxic carcinogen, it is unsuitable for clinical use. One treatment that has shown promise as a terminal sterilisation procedure is ethanol disinfection, as it has demonstrated effective decontamination of 1.5 mm thick alginate hydrogels following a 20-minute wash in 70% ethanol solution. Additionally, it allowed the mechanical and structural properties of the gel to be maintained and offers a cost-effective, but practical solution for terminal sterilisation of alginate-based biomaterials [117]. Therefore, future work will require examination of this procedure for use with alginate fluid gels, to determine its suitability and efficacy.

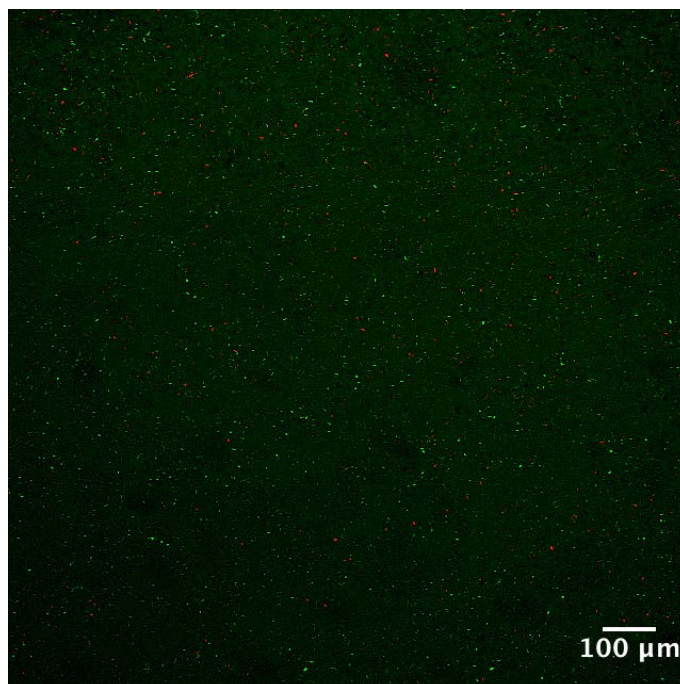


Figure 4.9: Calcein-AM/PI live/dead staining of BMAC cells in 2% w/v alginate fluid gel, cross-linked with 0.1M CaCl_2 , after 7 days. Live and dead cells stain green and red, respectively, with the majority of cells remaining viable following 7 days of culture within the fluid gel matrix.

4.3 Concluding statement

Alginate fluid gels of varying weight percentage were formulated using different production profiles that displayed desirable functional properties in terms of their injectability. Although, as could be anticipated, the 2% gel system demonstrated greater retention within model defects and superior self-setting ability as a result of its increased shear-viscosity profile. Therefore, this type of gel may be preferential in a clinical setting, where minimal operative time would be favourable and would also minimise the risk of infection at the defect site. Following analysis of the fluid gel microstructure, it was revealed that there appears to be an alignment of strands or fibres within the gel network that may have a direct influence on its mechanical properties. However, following preliminary experiments on the rheological properties of gels 48 hours post-formulation, there was a 10-20% reduction in the recorded storage modulus for 2% alginate fluid gels produced using two different formulation procedures, thus highlighting the

importance of conducting future degradation studies on these types of gels.

Finally, following the incorporation of an MC3T3 fibroblast cell population within alginate fluid gels of varying weight percentage, the majority of cells expressed excellent viability over a 7-day culture period and similar results were also seen with a population of human BMAC cells. Whilst the results from these initial studies are promising, they emphasise the need to determine the suitability and efficacy of terminal sterilisation procedures for alginate-based biomaterials in order to sufficiently eliminate the presence of bacteria for clinical use, as these types of gel cannot currently be manufactured under sterile conditions.

CHAPTER 5

RESULTS CHAPTER 2: TAILORING RELEASE OF KARTOGENIN AND THE BIOLOGICAL EFFECTS ON A HETEROGENEOUS CELL POPULATION WITHIN BMAC

As previously mentioned in Chapter 1, a therapeutic molecule, known as kartogenin (KGN), has been shown to stimulate selective chondrogenic differentiation of stem cells, which could therefore be favourable in facilitating differentiation of progenitor cells when incorporated into the fluid gel microenvironment. Consequently, studying the tailored release of this molecule from alginate fluid gel scaffolds was investigated in this chapter, along with analysis of metabolic activity by two different progenitor cell populations following external addition of KGN.

5.1 Materials and Methods

5.1.1 Materials

KGN and phosphate buffered saline (PBS) solution were purchased from Sigma-Aldrich and DMSO was obtained from Fisher Scientific.

Chondrogenic media

DMEM/F12 ((1:1)(1X), Gibco 21331-020, Life Technologies, UK) with 1%vol, ITS-X (Gibco 51500-056, Life Technologies, UK), 2.4%vol HEPES Buffer (H0887, Sigma Aldrich, UK), 2.4%vol L-Glutamine (G7513, Sigma Aldrich, UK), 1%vol Penicillin/Streptomycin (P4333-

100ml Sigma-Aldrich, UK), 100 nM Dexamethasone (Sigma-Aldrich D4902-100mg, UK), 27.5 $\mu\text{g/ml}$ Ascorbic Acid (2-phospho-L-ascorbic acid (49752-10G, Sigma-Aldrich, UK), 1.25 $\mu\text{g/ml}$ Bovine Serum Albumin (A8806-1G, Sigma-Aldrich, UK) and 10 ng/ml TGF- β 1 (PHG9214, Life Technologies).

Non-chondrogenic media

DMEM/F12 ((1:1)(1X), Gibco 21331-020, Life Technologies, UK) with 10% Fetal Bovine Serum (FBS) (Sigma-Aldrich F7524, UK), 2.4%vol HEPES Buffer (H088, Sigma-Aldrich, UK), 2.4%vol L-Glutamine (G7513, Sigma-Aldrich, UK), 1%vol Penicillin/Streptomycin (P4333-100ml Sigma-Aldrich, UK).

5.1.2 Preparation of KGN fluid gel

A 1 mM KGN stock solution was prepared by dissolving 15.5 mg KGN in 50 ml DMSO. KGN fluid gel was then produced by adding 30 μL of 1 mM KGN stock solution to the concentric cylinder after the alginate solution during the fluid gel formulation process, described in 4.1.

5.1.3 *In vitro* release study

The release profile of KGN from fluid gel was determined by placing 1g of 2% alginate fluid gel in 3 mL PBS solution, extracting 2.5ml of ageing media after 1hr, 12hrs, 24hrs and then 2, 3, 4, 5, 6, 7 days. The overall concentration of KGN in the fluid gel was $1\mu\text{molL}^{-1}$. KGN content in the liquid was estimated by absorbance at 277.8nm against a calibration curve using ultraviolet-visible (UV-vis) spectrophotometry.

5.1.4 *In vitro* chondrogenic differentiation of rat bone marrow stromal cells

Rat bone marrow stromal cells (rBMSCs) at passage 2 were seeded into 6-well plates at a density of 9.62×10^4 cells per well, left to attach over 48 hours and exposed to varying con-

centrations of KGN (0 nmolL^{-1} - $1 \text{ } \mu\text{molL}^{-1}$) through delivery in solution or via a 2% alginate fluid gel matrix, crosslinked with 0.1 M calcium chloride. The cells were then supplied with fresh high-glucose Dulbecco's modified Eagle's medium (DMEM) with 10% FBS, 1% vol Penicillin/Streptomycin, and KGN doses every 3 days. Cells were cultured at 37°C in 5% CO_2 .

5.1.5 Histology

Following 14 days of treatment, the media was then removed so that the cells could be fixed with ice cold 75% ethanol and subsequently stained for the detection of proteoglycans and collagen within the culture plate wells with Safranin O solution and later Alcian blue (1% in 3% acetic acid, pH 2.5, Sigma-Aldrich, UK).

5.1.6 *In vitro* chondrogenic differentiation of BM mononuclear cells

Following extraction from the ipsilateral iliac crest, heparinised bone marrow aspirate was filtered and concentrated using the Harvest BMAC[®], SmartPrep2[®] System. The BMAC samples were then analysed *in vitro*, where they were cultured in 6-well plates, at 37°C , 5% CO_2 in CO_2 incubator, with 500 μL of BMAC per well. Consistent volumes of BMAC were used as opposed to a definitive concentration of mono-nucleated cells, as this was more reflective of clinical practice [87]. The experiment was carried out in duplicate, as a result of infection developing in the third 6-well plate, and non-chondrogenic medium was used until cells became confluent, when it was exchanged with either fresh non-chondrogenic medium, chondrogenic medium, or non-chondrogenic medium supplemented with 100 nM, 200 nM or 400 nM of KGN (dissolved in DMSO and further diluted using non-chondrogenic medium), thereby removing any immunological and haematopoietic cells. This process was repeated every 2-3 days, with spent media collected and frozen at -20°C until assays were performed. As an additional control, a population of hBMSCs were isolated and expanded from bone chips removed from the femoral neck/head or tibial plateau, then subsequently plated at 1×10^5 cells per well at passage 2.

5.1.7 GAG contents analysis

After a 21-day culture period, chondrogenesis was evaluated quantitatively using Blyscan™ Sulfated Glycosaminoglycan Assay kit (Biocolor, Northern Ireland, UK). Sample absorbance was measured within 96-well plates in triplicate, at a wavelength of 630 nm using a microplate spectrophotometer. Cells were also examined for proteoglycan synthesis by staining with Alcian blue (1% in 3% acetic acid, pH 2.5, Sigma-Aldrich, UK). Briefly, cells were washed twice with PBS before being fixed in 4% paraformaldehyde (PFA) for 15 minutes at room temperature. In sequence, cells were rinsed 3 times with PBS and stained with Alcian blue (1% in 3% acetic acid, pH 2.5, Sigma-Aldrich, UK) for 30 minutes. Following this, cells were washed 3 times with 3% acetic acid for 2 minutes each and rinsed with dH₂O.

5.2 Results and discussion

5.2.1 Sustained KGN release from 2% alginate fluid gel over 7 days

The release profile of KGN incorporated within 2% w/v fluid gel system over a 7-day period was determined. Preliminary testing involved analysing the absorbance spectrum of KGN heated to 60°C alongside that of unheated KGN in DMSO solution. The results were indistinguishable and thus, the conclusion was drawn that incorporation of KGN within the formulation process would most likely not have an effect on its chemical activity. However, more formal analysis of the structure of the molecule will need to be undertaken in the future. Subsequently, a 2% alginate fluid gel was produced with an overall KGN concentration of 1 μ M, of which the release profile was determined by placing 1g of gel in 2.5ml of PBS, extracting the total volume of ageing media after 1hr, 12hrs, 24hrs and then 2, 3, 4, 5, 6, 7 days (Fig. 5.2). The KGN content in the liquid was then estimated by absorbance at 277.8nm against a calibration curve (Fig. 5.1) using UV-vis spectrophotometry.

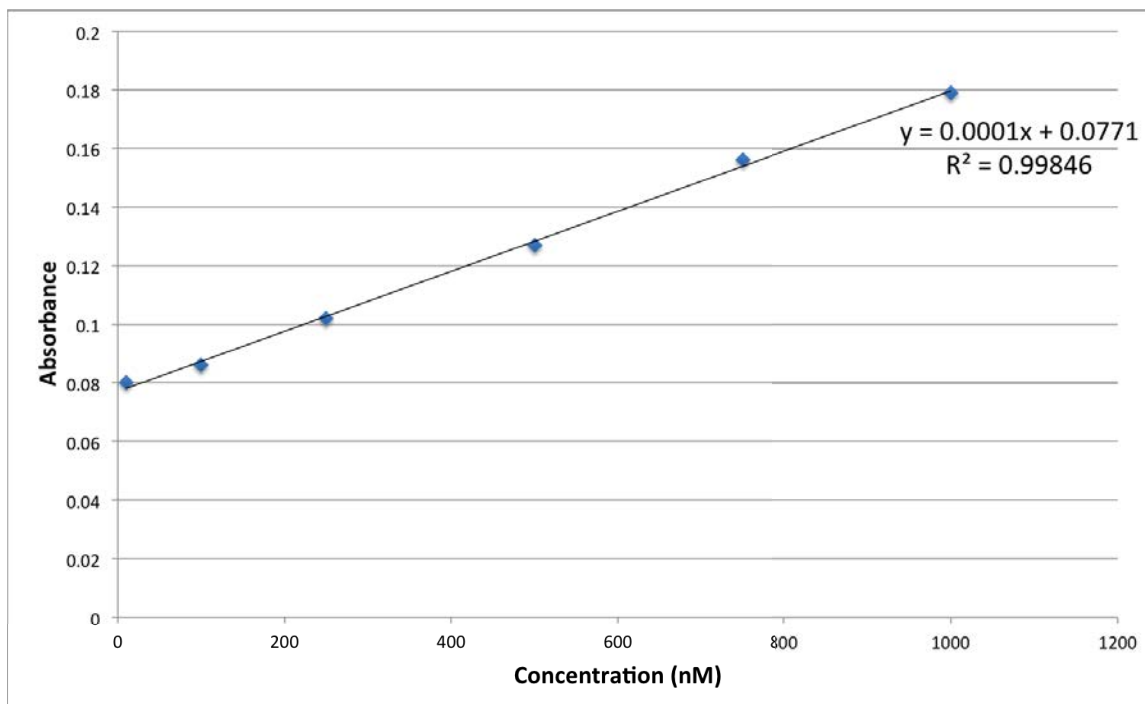


Figure 5.1: Calibration curve of KGN concentration against absorbance at 277.8nm using UV-vis spectrophotometry.

From Figure 5.2, there is no evidence of burst release of KGN from the gel, as initial release is below detectable levels. There is, however, slow release of KGN after 24 hours, which steadily increases for up to 96 hours, allowing faster release compared to other gel systems [14]. This lack of immediate burst release is unusual, but promising with regard to clinical application. Although, it is clear that there are some issues with this assay, as it indicates that after 72 hours, concentrations greater than that which was initially incorporated into the gel (1 mM of KGN), are being released. This is a result of possible DMSO and CaCl_2 release from the gel; after only a few hours, the release media appears to be composed of two immiscible liquids creating a blurriness of white light through the cuvette. This contributed approximately 0.170 in absorbance, which is highly significant. However, following 1-2 hours post transfer to the cuvette, the effect had dissipated leaving a clear liquid. These effects have been calibrated against, although future experiments may account for this by allowing 1-2 hours before taking the final absorbance measurement. There is also the possibility that precipitation of the CaCl_2 with the PBS release media is occurring, which was explored through accelerated ageing experiments that mimicked

the breakdown of the gel over days, by measuring the absorbance of 3mM of CaCl_2 in 3mL of PBS. This resulted in clear formation of precipitates in the release media, with simulated burst release of all the CaCl_2 from 1mL of fluid gel causing significant clouding. Clearly, this would invalidate any samples measured using UV-vis spectrophotometry, as the Beer-Lambert law only holds for analytes that are homogeneously distributed in the media and the precipitates cannot be modelled or calibrated out. Therefore, in future studies, it will be necessary to make notes on sample turbidity and the presence of precipitates in test runs, otherwise it may be more suitable to use an alternative release medium to PBS, if precipitates are observed at longer time points.

An additional observation that was made was the sensitivity of the assay to small changes in KGN concentration, which was illustrated by only a 0.1 change in absorbance covering the 250nM to 1000nM concentration range. Therefore, great care must be taken in handling the sources of error in preparing the KGN solution. Furthermore, the calibration curve helped clarify an estimate of the lower limit of detection (LLOD) for KGN in the region of 10-100nM, as there is no change in absorbance between 1nM and 10nM (both have absorbance values of 0.08). Thus, this leads to the conclusion that the LLOD for the assay will be at least 10nM, though its precise value is yet to be determined and explains why the calibration curve plateaus at low concentrations of KGN release in the samples. This can also be seen in the case of the first time point in the KGN release figure, which is out of the detection range.

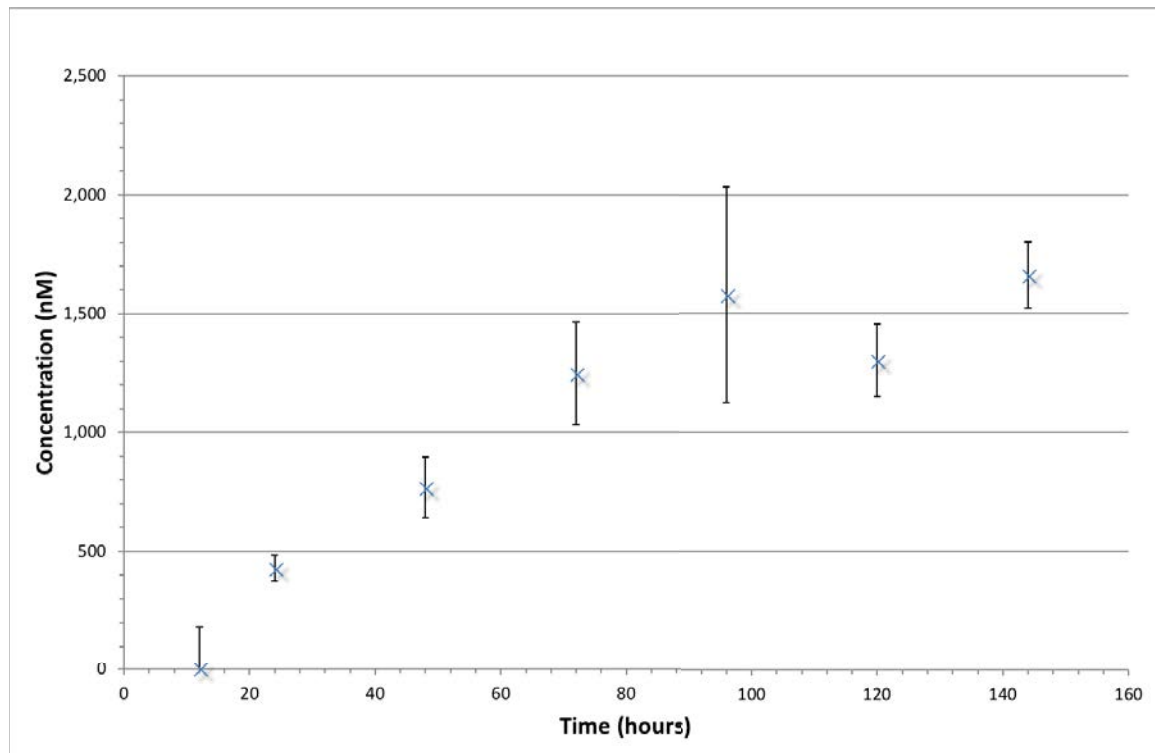


Figure 5.2: Sustained KGN release from 2% alginate fluid gel over 7 days in PBS media, with continuous slow release of KGN following 24 hours.

5.2.2 Safranin O and Alcian blue staining of rBMSC's following 14 days culture and treatment with KGN

One of the key objectives is to deliver and maintain the viability of a progenitor cell population, which has been successfully achieved through incorporation of a rat bone marrow stromal cell (rBMSC) population within the fluid gel matrix, with metabolic activity being assessed through analysis of cartilage matrix production following external addition of KGN. As illustrated in Figure 5.3, over a 14-day period and following staining with Safranin O and Alcian Blue solution, production of both proteoglycans and collagen was observed, with evidence of costaining in some regions that suggests structuring of an organised matrix by rat bone marrow stromal cells (rBMSCs), particularly at 10nM.

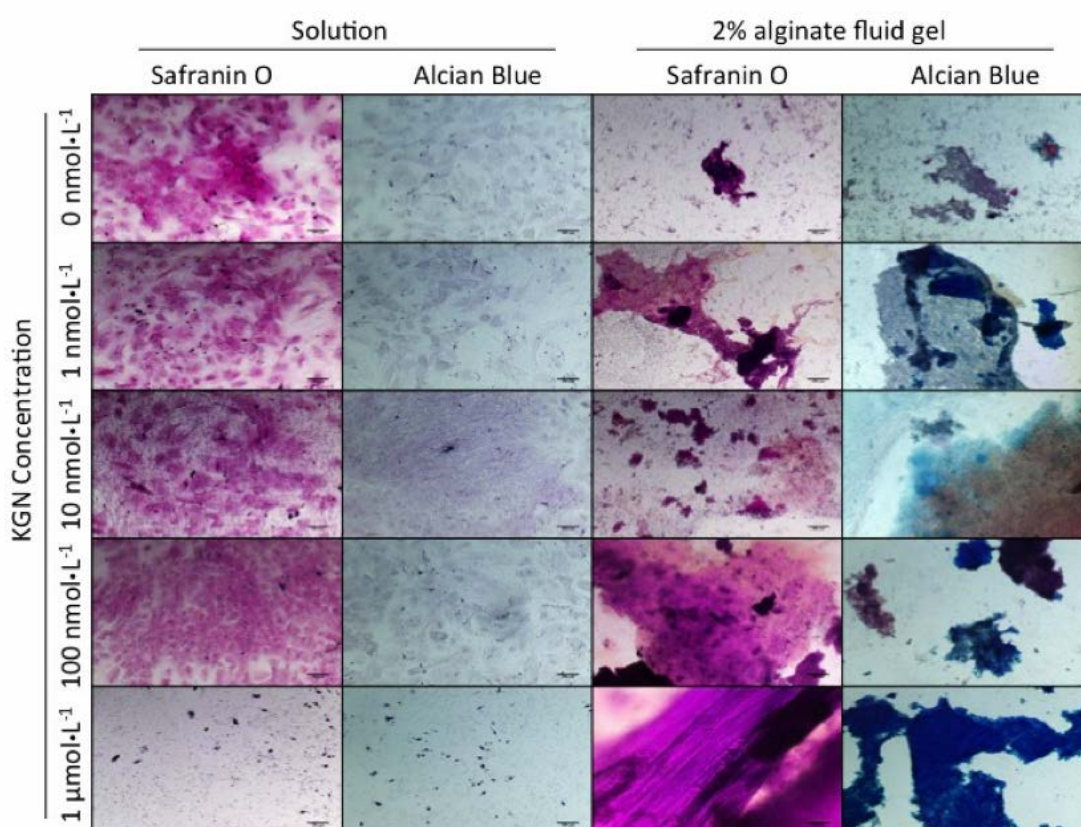


Figure 5.3: Safranin O and Alcian Blue staining of rBMSC's following 14 days of treatment with KGN, illustrating production of both proteoglycans and collagen, with evidence of costaining suggesting structuring of an organised matrix, particularly at 10nM.

5.2.3 DMMB assay and Alcian blue staining of BMAC and hBM-MSC cells following 21 days culture and treatment with KGN

Proceeding from the investigation of rBMSCs, following 14 days of treatment with KGN, a similar study was undertaken to examine the effect of KGN on BMAC in comparison to a population of human BM-MSCs (hBM-MSCs), as a positive control. Effective known doses of KGN in non-chondrogenic media were delivered over a 21-day chondrogenic culture period, within 6-well plates and chondrogenesis was determined using both Alcian blue staining and a DMMB assay to identify the production of proteoglycans. Promisingly, brightfield images indicated a large proportion of the BMAC and hBM-MSC cells were alive following the 21-day chondrogenic culture period (Fig. 5.4 and Fig. 5.5).

The results shown in Figures 5.6 illustrate the effect of 100nM KGN treatment on hBM-MSCs and BMAC, over a 21-day period, with higher GAG concentrations being detected at days 0, 7 and 21, following the collection of spent media from cultured BMAC cells. Similar results were seen following 200nM KGN treatment (5.7), although there were only minor changes in GAG concentration for each cell type over the 21-day period. In Figure 5.8, there were greater changes in GAG concentration, following 400nM KGN treatment, with the largest increase being seen on day 14 in hBM-MSC cells. Although, this may be a result of the larger errors in measurement at this concentration. This is also evident in Figure 5.9, where 400nM KGN treatment appears to have the greatest influence on GAG production in hBM-MSCs after 14 days culture. However, the results for treatment with 100nM KGN were more consistent, with increases in GAG concentration being measured gradually up to day 21, when they decreased, possibly due to cell apoptosis from a minor infection developing in wells containing hBM-MSCs. Additionally, BMAC cells responded favourably to treatment with 100nM KGN, as illustrated in Figure 5.10, followed closely by treatment with chondrogenic media, though it was clear there were similar decreases in GAG concentration by day 21. Visual staining of proteoglycans by Alcian blue can also be seen in Figure 5.11, however there was generally minimal staining across both sets of plates.

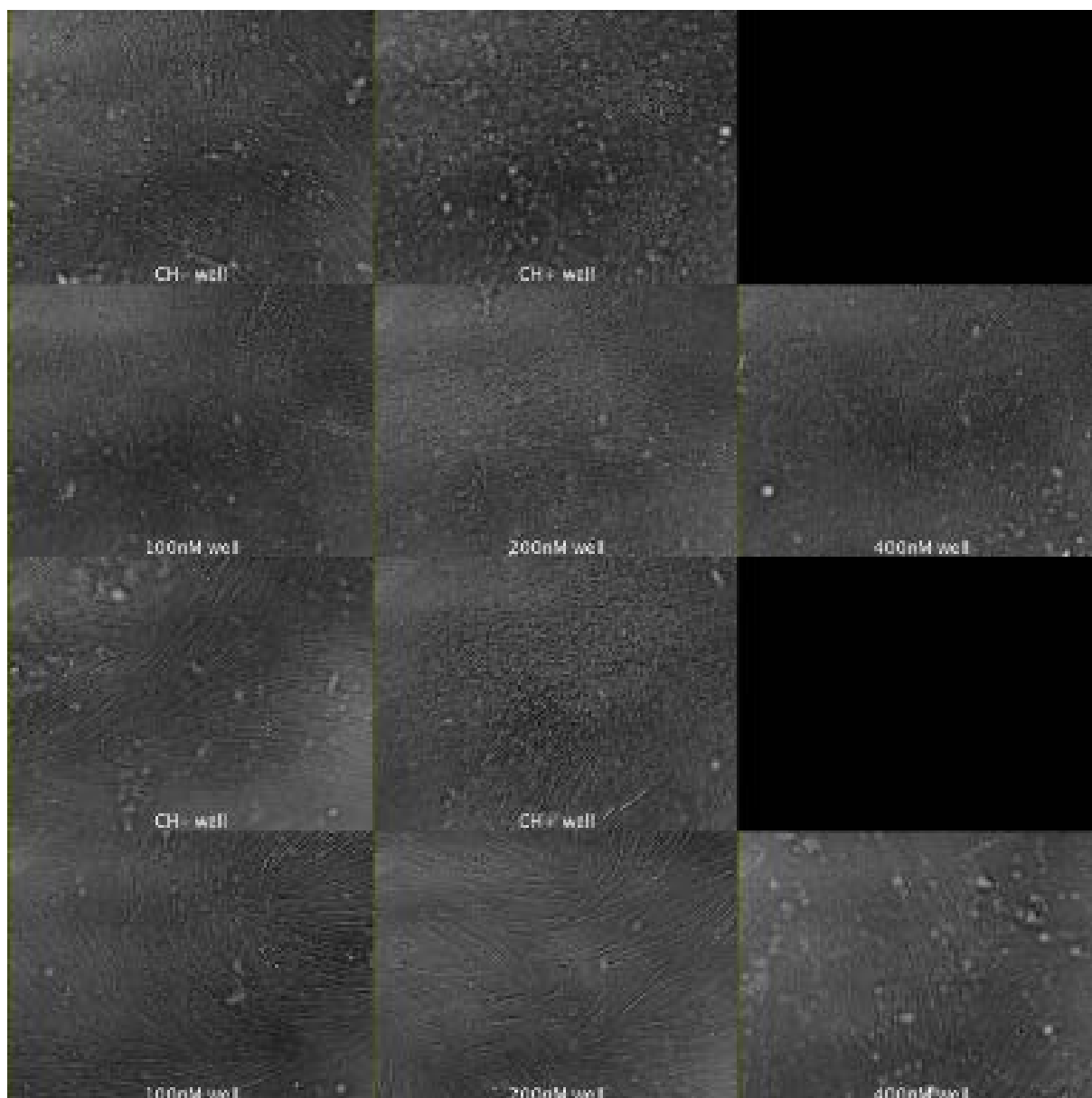


Figure 5.4: Brightfield images of unstained cells indicate that the majority of BMAC cells were alive after approximately 21 days of culture. Abbreviations used: non-chondrogenic medium (CH-), chondrogenic medium (CH+), non-chondrogenic medium supplemented with 100 nM (100nM), 200 nM (200nM) or 400 nM (400nM) of KGN (dissolved in DMSO and further diluted using non-chondrogenic medium).

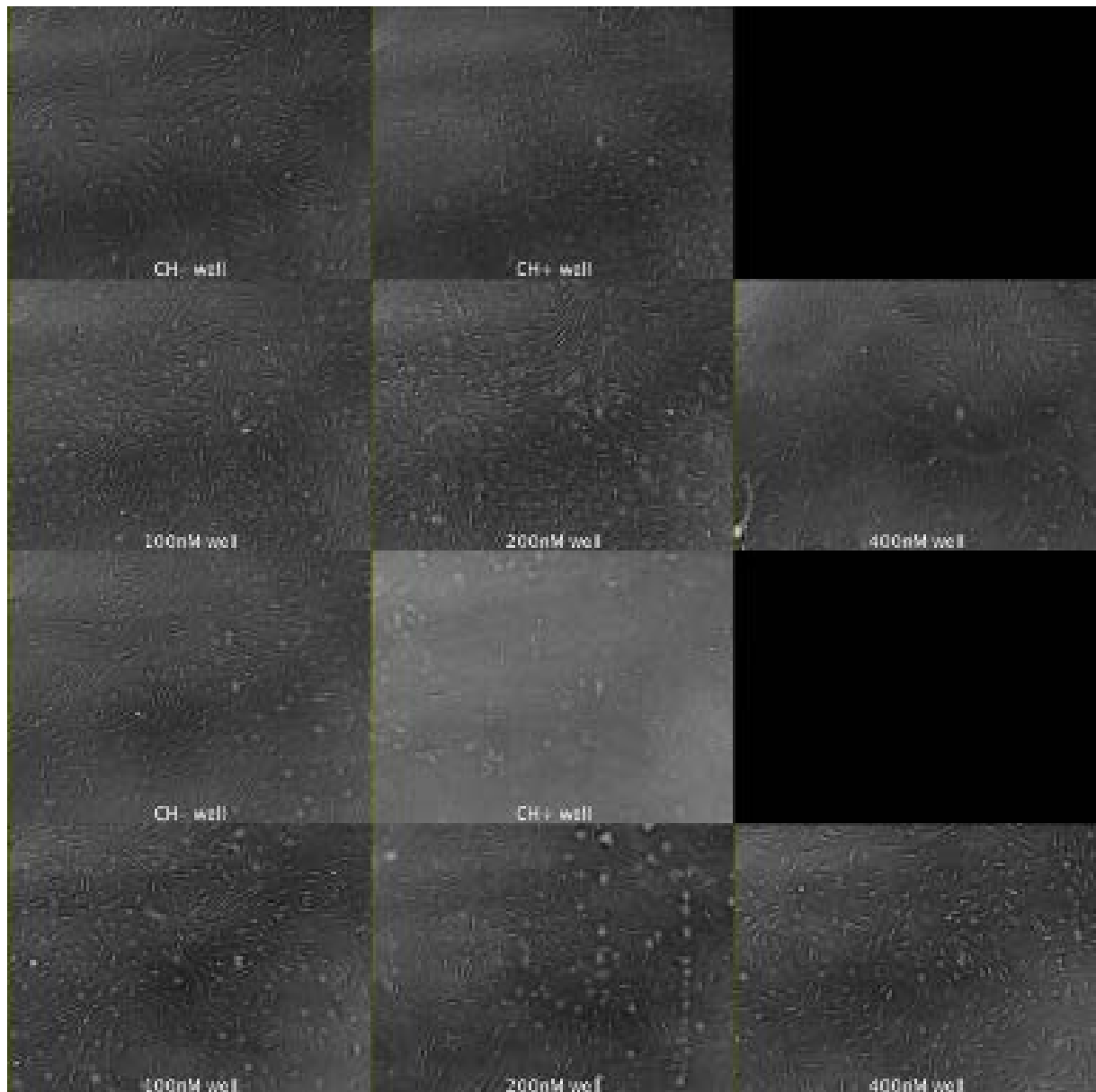


Figure 5.5: Brightfield images of unstained cells indicate that the majority of hBM-MSC cells were alive after approximately 21 days of culture. Abbreviations used: non-chondrogenic medium (CH-), chondrogenic medium (CH+), non-chondrogenic medium supplemented with 100 nM (100nM), 200 nM (200nM) or 400 nM (400nM) of KGN (dissolved in DMSO and further diluted using non-chondrogenic medium).

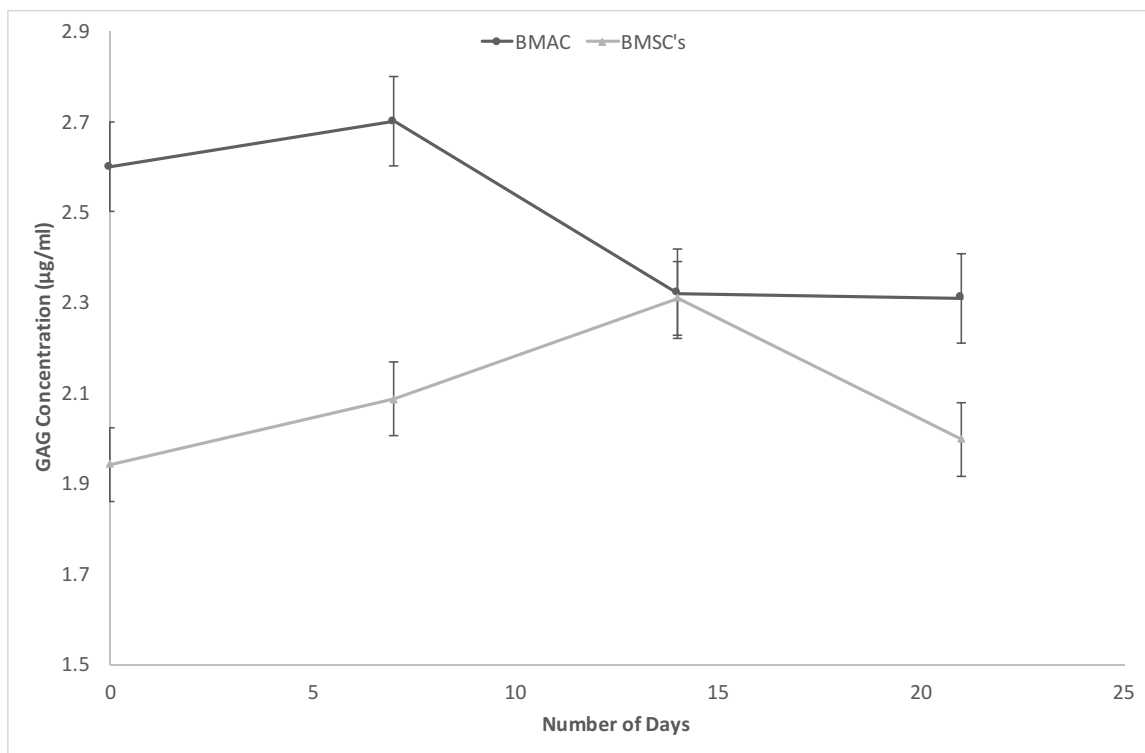


Figure 5.6: DMMB assay results following the treatment of hBM-MSCs and BMAC with 100nM of KGN over 21 days.

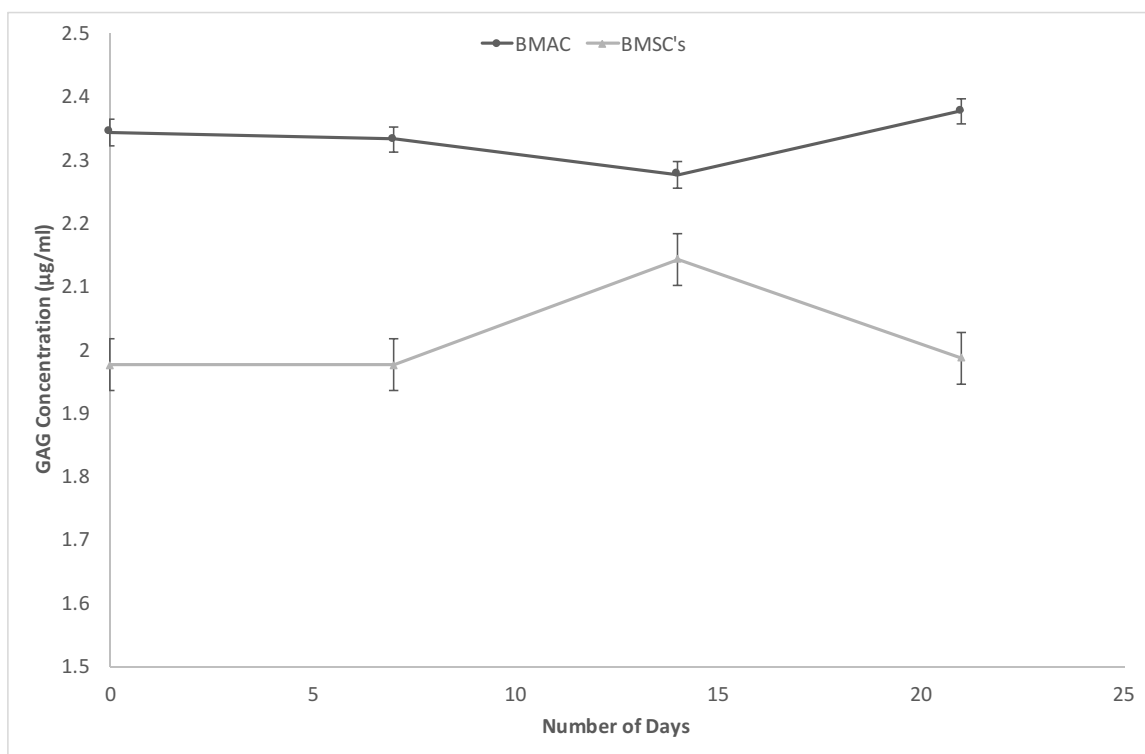


Figure 5.7: DMMB assay results following the treatment of hBM-MSCs and BMAC with 200nM of KGN over 21 days.

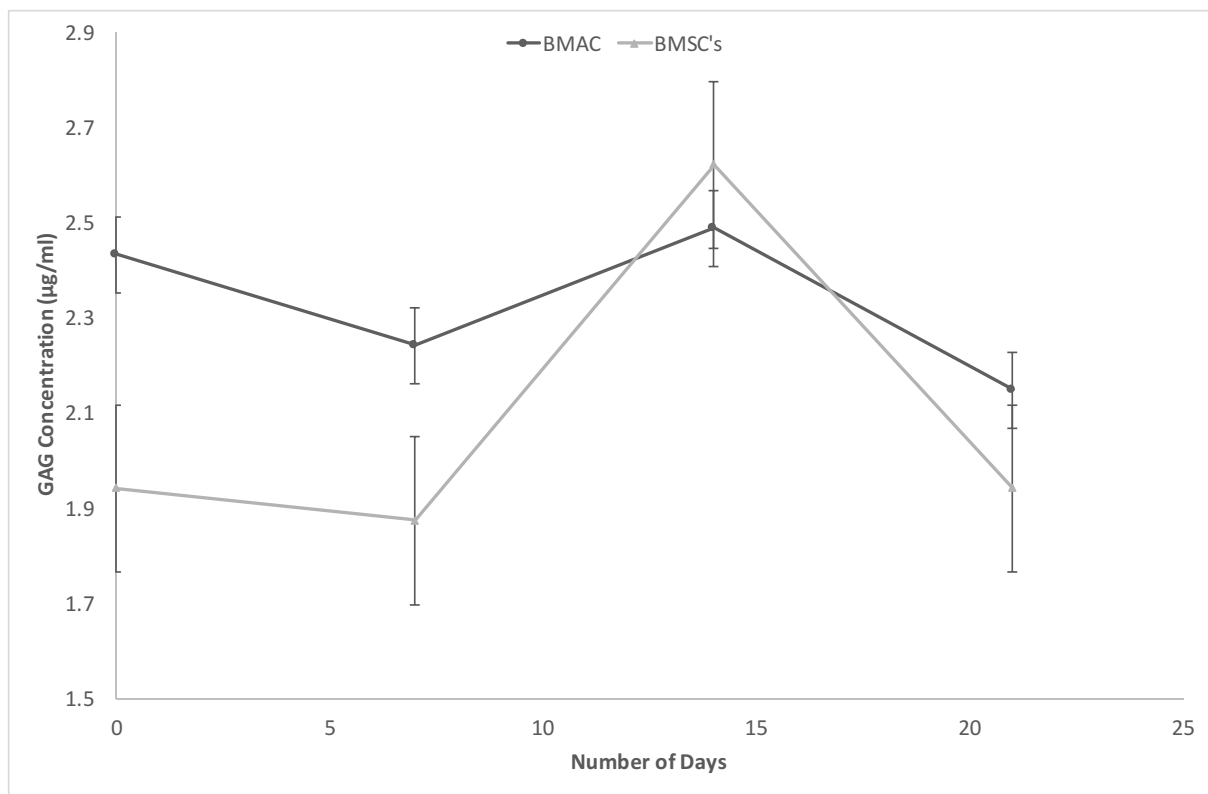


Figure 5.8: DDMMB assay results following the treatment of hBM-MSCs and BMAC with 400nM of KGN over 21 days.

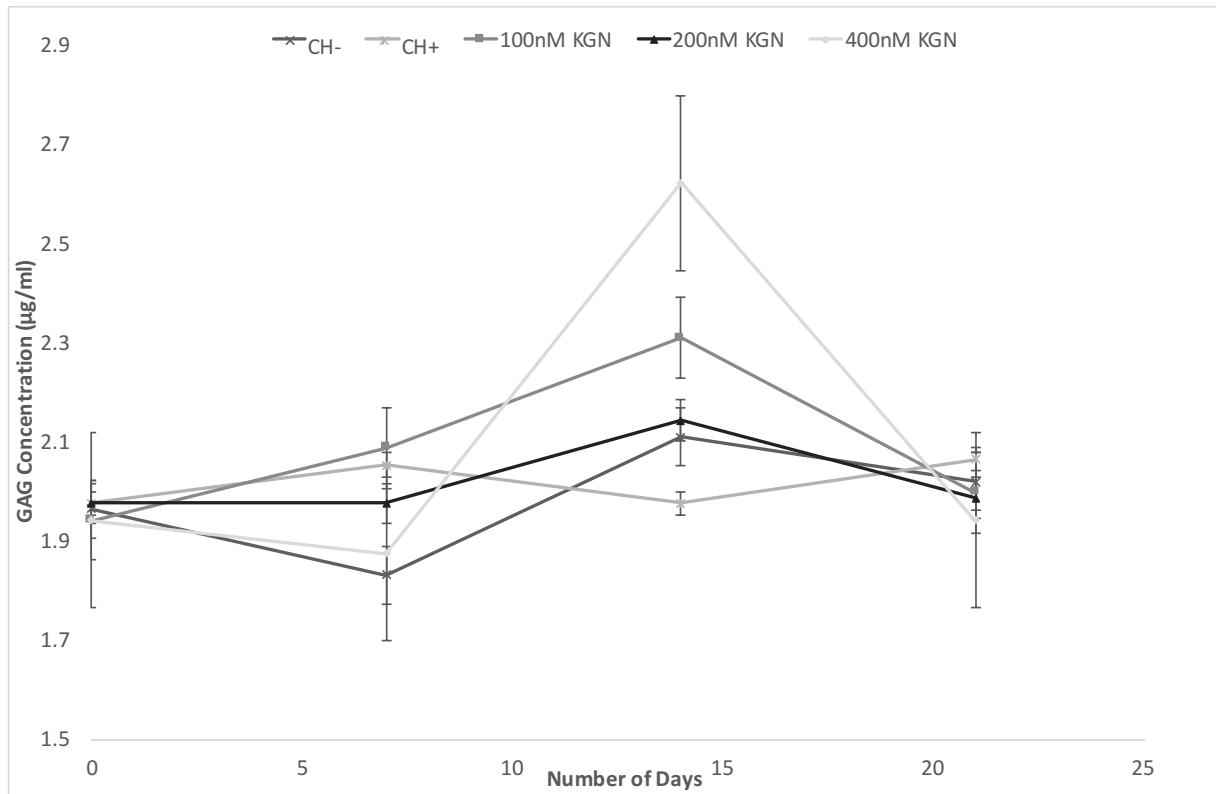


Figure 5.9: DMMB assay results following the treatment of hBM-MSCs with varying concentrations of KGN over 21 days. Abbreviations used: non-chondrogenic medium (CH-), chondrogenic medium (CH+), non-chondrogenic medium supplemented with 100 nM (100nM), 200 nM (200nM) or 400 nM (400nM) of KGN (dissolved in DMSO and further diluted using non-chondrogenic medium).

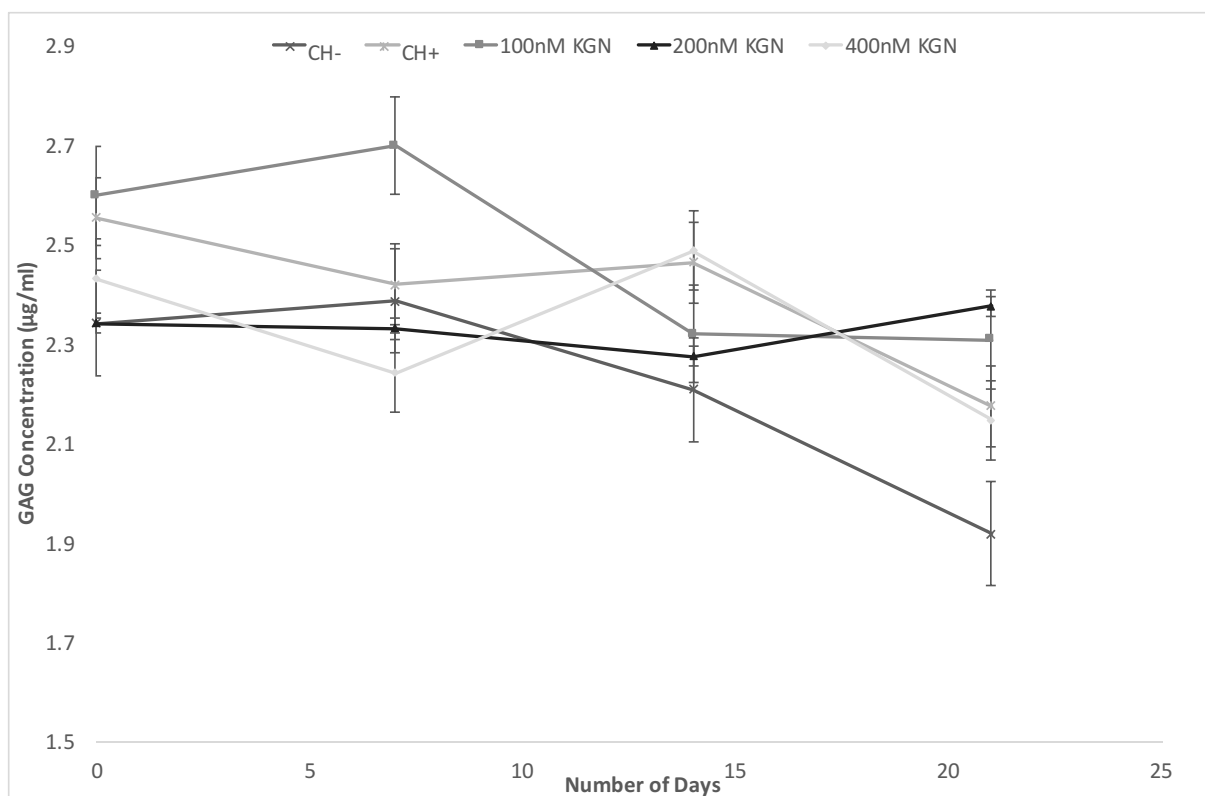
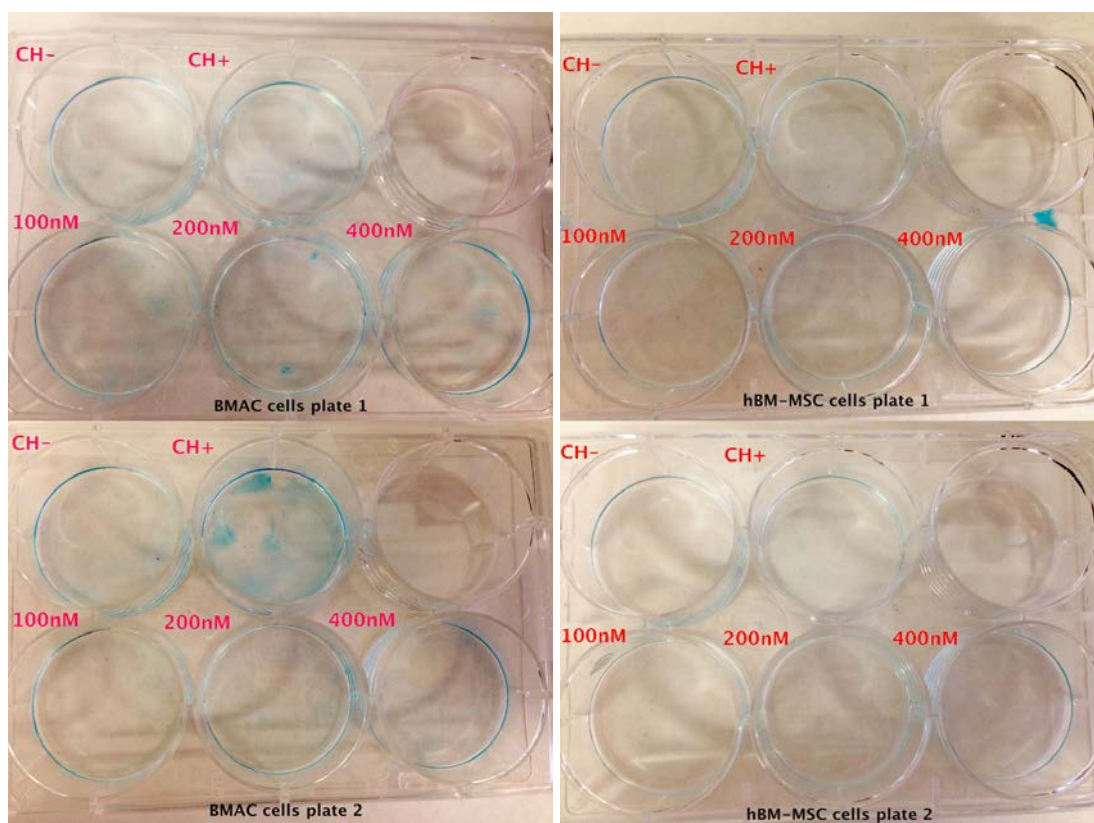


Figure 5.10: DMMB assay results following the treatment of BMAC with varying concentrations of KGN over 21 days. Abbreviations used: non-chondrogenic medium (CH-), chondrogenic medium (CH+), non-chondrogenic medium supplemented with 100 nM (100nM), 200 nM (200nM) or 400 nM (400nM) of KGN (dissolved in DMSO and further diluted using non-chondrogenic medium).



(a) BMAC plates

(b) hBM-MSC plates

Figure 5.11: Alcian blue staining of proteoglycans produced by BMAC and hBM-MSC cells. Abbreviations used: non-chondrogenic medium (CH-), chondrogenic medium (CH+), non-chondrogenic medium supplemented with 100 nM (100nM), 200 nM (200nM) or 400 nM (400nM) of KGN (dissolved in DMSO and further diluted using non-chondrogenic medium).

Overall, the results from the DMMB assay of hBM-MSC and BMAC cells demonstrated a marginal increase in GAG concentration produced by cells within the BMAC population compared to the hBMSC population, although statistically there was no significant difference between the different sample populations for BMAC and hBM-MSCs. Despite noticing some infection in the chondrogenic wells of the plates containing hBM-MSCs, it seems clear from the light microscope images shown in Figures 5.4 and 5.5 that the majority of cells across both sets of plates remained viable after 21 days of culture. Still, there appears to be a difference between in confluency, with the hBM-MSCs appearing less confluent than the population of BMAC cells. This could have been a result of the infection in the wells containing hBM-MSCs, or it could be that chondrogenesis was induced prior to hBM-MSCs becoming fully conflu-

ent. Altogether, these results were attributed to the 2D culture environment and conditions used with the aim of enabling minimal manipulation of BMAC samples prior to culturing, whereas chondrogenic differentiation of MSCs is primarily carried out using micromass pellet culture to create and provide a three-dimensional hypoxic environment that facilitates cell-cell interactions, which recapitulates pre-chondrogenic condensations experienced in the early stages of embryonic development. This could elucidate the decreasing trend in GAG concentration seen for both hBM-MSC and BMAC cells, as cells differentiate along a more fibroblastic phenotype. Reduction in oxygen tension is also a key element in stimulating the production of VEGF through hypoxic inducible factor (HIF-1), highlighting its significance in cartilage growth, as VEGF reportedly enhances cell viability via expression of anti-apoptotic molecules [118, 81].

5.3 Concluding statement

A therapeutic molecule, known as kartogenin (KGN), that has been shown to stimulate selective chondrogenic differentiation of stem cells, was successfully incorporated into an alginate fluid gel scaffold and displayed a steady release profile over a 7-day period. The system exhibited a lack of immediate burst release, which, though unusual, is promising with regard to clinical application. However, there were some clear issues with the assay, indicating higher concentrations of KGN being released from the gel than were actually incorporated. This was possibly caused by the formation of precipitates from the CaCl_2 present within the gel and thus, invalidated any samples measured using UV-vis spectrophotometry, due to invalidation of the Beer-Lambert law. Future work may therefore consider the use of a more suitable release medium to PBS, as well as the use of high performance liquid chromatography (HPLC), which is more sensitive for assaying small changes in concentration.

Subsequent to the release studies with KGN, the metabolic activity of two different progenitor cell populations within the fluid gel matrix were assessed following external addition of KGN. Firstly, analysis of cartilage matrix production by a rat bone marrow stromal cell (rBMSC)

population was assessed over a 14-day culture period, displaying evidence of proteoglycan and collagen production, particularly at 10nM. Further work then compared the effect of KGN on both human BMAC and BM-MSC (hBM-MSC) cell populations over a 21-day culture period. Promisingly, a substantial proportion of cells appeared to be alive following the 21-day chondrogenic culture period, although statistically there was no significant difference in proteoglycan production between the different sample populations for BMAC and hBM-MSCs. Altogether, these results were attributed to the 2D culture environment and conditions used with the aim of enabling minimal manipulation of BMAC samples prior to culturing, whereas chondrogenic differentiation of MSCs is primarily carried out using micromass pellet culture to create and provide a three-dimensional hypoxic environment that facilitates cell-cell interactions, which recapitulates pre-chondrogenic condensations experienced in the early stages of embryonic development. In summary, this illustrates the importance of constructing a simulative culture system to enable a three-dimensional extracellular matrix to develop, as it is clear that the other two prerequisites of chondrogenesis; addition of serum-free medium and a TGF-isoform, are conditional upon this requirement [102].

CHAPTER 6

CONCLUSIONS AND FUTURE WORK

6.1 Conclusions

This work has involved the development of a self-setting gel system for kartogenin delivery in the form of an injectable alginate fluid-gel microenvironment and scaffold that is capable of supporting cell viability and be retained within model defects. This biomaterial can be formulated to steadily release effective known doses of KGN over a 7-day period, although there were notably some issues with the assay using UV-vis spectrophotometry, due to invalidation of the Beer-Lambert Law. Therefore, future work could consider the use of a more suitable release medium to PBS, as well as the use of high performance liquid chromatography (HPLC), which is more sensitive for assaying small changes in concentration. Finally, the potential of the fluid gel microenvironment in promoting the chondrogenic differentiation of BMSCs and a heterogeneous BMAC cell population demonstrated initial promise, though further work is needed to corroborate these preliminary findings.

6.2 Recommendations for future work

Future work will include further characterisation of the fluid gel microstructure, through both phase contrast and confocal microscopy by fluorescently labelling the alginate biopolymer. Additionally, it is important that the effect of KGN on BMAC in comparison to a population of human BM-MSCs (hBM-MSCs) is reassessed using micromass pellet culture, in order to formally determine whether the existing results can be indeed be attributed to the 2D culture

environment and conditions that were used. As previously mentioned, it will also be essential to conduct long term degradation studies of the fluid gel systems, which was highlighted during the mechanical testing process, as this will clearly impact the retention and metabolic activity of delivered cells at the defect site during the healing process.

Further down the line, it will be necessary to examine methods of terminal sterilisation for the cell delivery vehicle, specifically prolonged UV irradiation, for example 24- or 48-hour exposure, as well as ethanol disinfection. Finally, it would be beneficial to explore refinement of the gel formulation, in order to achieve a more homogenous structure, which may be achievable through utilising pH sensitive Ca^{2+} chelates, such as CaEDTA, allowing slower gelation kinetics [119].

LIST OF REFERENCES

- [1] S. Macmull, J. Skinner, G. Bentley, R. Carrington, T. Briggs *et al.*, “Treating articular cartilage injuries of the knee in young people,” *BMJ [online]*, vol. 340, p. c998, 2010.
- [2] *NICE consults on research recommendation for knee cartilage treatment*. National Institute for Health and Care Excellence (NICE), 2015. [Online]. Available: <https://www.nice.org.uk/news/press-and-media/nice-consults-on-research-recommendation-for-knee-cartilage-treatment>
- [3] R. Bitton, “The economic burden of osteoarthritis.” *The American journal of managed care*, vol. 15, no. 8 Suppl, pp. S230–S3255, 2009.
- [4] P. Orth, A. Rey-Rico, J. K. Venkatesan, H. Madry, and M. Cucchiaroni, “Current perspectives in stem cell research for knee cartilage repair,” *Stem cells and cloning: advances and applications*, vol. 7, pp. 1–17, 2014.
- [5] A. J. S. Fox, A. Bedi, and S. A. Rodeo, “The basic science of articular cartilage: structure, composition, and function,” *Sports Health: A Multidisciplinary Approach*, vol. 1, no. 6, pp. 461–468, 2009.
- [6] *Articular cartilage restoration: A review of currently available methods*. New Orleans, Louisiana: Proceedings of the Seventy-Seventh Annual Meeting of the American Academy of Orthopaedic Surgeons, March 2010.
- [7] S. Araki, S. Imai, H. Ishigaki, T. Mimura, K. Nishizawa, H. Ueba, K. Kumagai, M. Kubo, K. Mori, K. Ogasawara *et al.*, “Improved quality of cartilage repair by bone marrow mesenchymal stem cells for treatment of an osteochondral defect in a cynomolgus macaque model,” *Acta orthopaedica*, vol. 86, no. 1, pp. 119–126, 2015.
- [8] *Cartilage damage - Treatment*, Department of Health - NHS Choices, 2015. [Online]. Available: <http://www.nhs.uk/Conditions/Cartilage-damage/Pages/Treatment.aspx>
- [9] H. Nejadnik, J. H. Hui, E. P. F. Choong, B.-C. Tai, and E. H. Lee, “Autologous bone marrow–derived mesenchymal stem cells versus autologous chondrocyte implantation

- an observational cohort study,” *The American journal of sports medicine*, vol. 38, no. 6, pp. 1110–1116, 2010.
- [10] *Reflection paper on classification of advanced therapy medicinal products*. London, UK: European Medicines Agency, 2014. [Online]. Available: http://www.ema.europa.eu/ema/index.jsp?curl=pages/regulation/general/general_content_000296.jsp&mid=WC0b01ac058007f4bc
 - [11] K. F. Pearce, M. Hildebrandt, H. Greinix, S. Scheding, U. Koehl, N. Worel, J. Apperley, M. Edinger, A. Hauser, E. Mischak-Weissinger *et al.*, “Regulation of advanced therapy medicinal products in europe and the role of academia,” *Cytotherapy*, vol. 16, no. 3, pp. 289–297, 2014.
 - [12] N. Devlin and D. Parkin, “Does nice have a cost-effectiveness threshold and what other factors influence its decisions? a binary choice analysis,” *Health Economics*, vol. 13, no. 5, pp. 437–452, 2004.
 - [13] K. Johnson, S. Zhu, M. S. Tremblay, J. N. Payette, J. Wang, L. C. Bouchez, S. Meeusen, A. Althage, C. Y. Cho, X. Wu *et al.*, “A stem cell–based approach to cartilage repair,” *Science*, vol. 336, no. 6082, pp. 717–721, 2012.
 - [14] X. Li, J. Ding, Z. Zhang, M. Yang, J. Yu, J. Wang, F. Chang, and X. Chen, “Kartogenin-incorporated thermogel supports stem cells for significant cartilage regeneration,” *ACS applied materials & interfaces*, vol. 8, no. 8, pp. 5148–5159, 2016.
 - [15] E. A. Makris, A. H. Gomoll, K. N. Malizos, J. C. Hu, and K. A. Athanasiou, “Repair and tissue engineering techniques for articular cartilage,” *Nature Reviews Rheumatology*, vol. 11, no. 1, pp. 21–34, 2015.
 - [16] Z. Cao, C. Dou, and S. Dong, “Scaffolding biomaterials for cartilage regeneration,” *Journal of Nanomaterials*, vol. 2014, p. 4, 2014.
 - [17] I. F. Farrés, R. Moakes, and I. Norton, “Designing biopolymer fluid gels: A microstructural approach,” *Food Hydrocolloids*, vol. 42, pp. 362–372, 2014.
 - [18] I. Norton, D. Jarvis, and T. Foster, “A molecular model for the formation and properties of fluid gels,” *International Journal of Biological Macromolecules*, vol. 26, no. 4, pp. 255–261, 1999.

- [19] J. A. Rowley, G. Madlambayan, and D. J. Mooney, "Alginate hydrogels as synthetic extracellular matrix materials," *Biomaterials*, vol. 20, no. 1, pp. 45–53, 1999.
- [20] K. Draget, G. Phillips, P. Williams *et al.*, "Alginates." *Handbook of hydrocolloids*, pp. 807–828, 2009.
- [21] J.-S. Yang, Y.-J. Xie, and W. He, "Research progress on chemical modification of alginate: A review," *Carbohydrate polymers*, vol. 84, no. 1, pp. 33–39, 2011.
- [22] S. N. Pawar and K. J. Edgar, "Alginate derivatization: a review of chemistry, properties and applications," *Biomaterials*, vol. 33, no. 11, pp. 3279–3305, 2012.
- [23] A. R. Short, D. Koralla, A. Deshmukh, B. Wissel, B. Stocker, M. Calhoun, D. Dean, and J. O. Winter, "Hydrogels that allow and facilitate bone repair, remodeling, and regeneration," *Journal of Materials Chemistry B*, vol. 3, no. 40, pp. 7818–7830, 2015.
- [24] N. Peppas and A. Mikos, "Preparation methods and structure of hydrogels," *Hydrogels in medicine and pharmacy*, vol. 1, pp. 1–27, 1986.
- [25] N. Peppas, P. Bures, W. Leobandung, and H. Ichikawa, "Hydrogels in pharmaceutical formulations," *European journal of pharmaceuticals and biopharmaceutics*, vol. 50, no. 1, pp. 27–46, 2000.
- [26] E. M. Ahmed, "Hydrogel: preparation, characterization, and applications," *Journal of advanced research*, 2013.
- [27] L. Brannon-Peppas and R. S. Harland, *Absorbent polymer technology*. Elsevier, 2012.
- [28] J. M. Saul and D. F. Williams, "12 - hydrogels in regenerative medicine," in *Handbook of Polymer Applications in Medicine and Medical Devices*, ser. Plastics Design Library, K. M. Ebnesajjad, Ed. Oxford: William Andrew Publishing, 2011, pp. 279 – 302. [Online]. Available: <http://www.sciencedirect.com/science/article/pii/B9780323228053000128>
- [29] A. S. Hoffman, "Hydrogels for biomedical applications," *Advanced Drug Delivery Reviews*, vol. 54, no. 1, pp. 3 – 12, 2002, recent Developments in Hydrogels. [Online]. Available: <http://www.sciencedirect.com/science/article/pii/S0169409X01002393>

- [30] M. Hacker and A. Mikos, "Chapter 33 - synthetic polymers," in *Principles of Regenerative Medicine (Second edition)*, second edition ed., A. A. L. A. T. Nerem, Ed. San Diego: Academic Press, 2011, pp. 587 – 622. [Online]. Available: <http://www.sciencedirect.com/science/article/pii/B9780123814227100331>
- [31] W. Zhao, X. Jin, Y. Cong, Y. Liu, and J. Fu, "Degradable natural polymer hydrogels for articular cartilage tissue engineering," *Journal of Chemical Technology and Biotechnology*, vol. 88, no. 3, pp. 327–339, 2013.
- [32] D. A. Garrec and I. T. Norton, "Understanding fluid gel formation and properties," *Journal of Food Engineering*, vol. 112, no. 3, pp. 175–182, 2012.
- [33] H. Kiani, M. Mousavi, and Z. Mousavi, "Particle stability in dilute fermented dairy drinks: Formation of fluid gel and impact on rheological properties," *Food Science and Technology International*, vol. 16, no. 6, pp. 543–551, 2010.
- [34] P. W. Cox, F. Spyropoulos, and I. T. Norton, "{CHAPTER} 6 - effect of processing on biopolymer interactions," in *Modern Biopolymer Science*, S. K. T. N. B. Ubbink, Ed. San Diego: Academic Press, 2009, pp. 199 – 224. [Online]. Available: <http://www.sciencedirect.com/science/article/pii/B9780123741950000069>
- [35] M. Djabourov, K. Nishinari, and S. B. Ross-Murphy, *Physical gels from biological and synthetic polymers*. Cambridge University Press, 2013.
- [36] D. Streather, "The development of a fluid-gel system to selectively bind specific cells from bone marrow to aid articular cartilage restoration," Master's thesis, University of Birmingham, 2015.
- [37] J. Hodgkins, "The development of a single-step bedside cell sorting delivery system to aid articular cartilage regeneration," Master's thesis, University of Birmingham, 2015.
- [38] A. Gabriele, F. Spyropoulos, and I. Norton, "Kinetic study of fluid gel formation and viscoelastic response with kappa-carrageenan," *Food Hydrocolloids*, vol. 23, no. 8, pp. 2054–2061, 2009.
- [39] G. Blaine, "Experimental observations on absorbable alginate products in surgery: gel, film, gauze and foam," *Annals of surgery*, vol. 125, no. 1, p. 102, 1947.
- [40] E. G. Passe and G. Blaine, "Alginates in endaural wound dressing," *The Lancet*, vol. 252, no. 6530, p. 651, 1948.

- [41] A. Al-Shamkhani and R. Duncan, "Radioiodination of alginate via covalently-bound tyrosinamide allows monitoring of its fate in vivo," *Journal of bioactive and compatible polymers*, vol. 10, no. 1, pp. 4–13, 1995.
- [42] J. Sun and H. Tan, "Alginate-based biomaterials for regenerative medicine applications," *Materials*, vol. 6, no. 4, pp. 1285–1309, 2013.
- [43] T. Gilchrist and A. Martin, "Wound treatment with sorbsan—an alginate fibre dressing," *Biomaterials*, vol. 4, no. 4, pp. 317–320, 1983.
- [44] A. Groves and J. Lawrence, "Alginate dressing as a donor site haemostat." *Annals of the Royal College of Surgeons of England*, vol. 68, no. 1, p. 27, 1986.
- [45] H. H. Tønnesen and J. Karlsen, "Alginate in drug delivery systems," *Drug development and industrial pharmacy*, vol. 28, no. 6, pp. 621–630, 2002.
- [46] M. S. Shoichet, R. H. Li, M. L. White, and S. R. Winn, "Stability of hydrogels used in cell encapsulation: An in vitro comparison of alginate and agarose," *Biotechnology and bioengineering*, vol. 50, no. 4, pp. 374–381, 1996.
- [47] K. H. Bouhadir, K. Y. Lee, E. Alsberg, K. L. Damm, K. W. Anderson, and D. J. Mooney, "Degradation of partially oxidized alginate and its potential application for tissue engineering," *Biotechnology progress*, vol. 17, no. 5, pp. 945–950, 2001.
- [48] J. Vanacker, V. Luyckx, M.-M. Dolmans, A. Des Rieux, J. Jaeger, A. Van Langendonck, J. Donnez, and C. A. Amorim, "Transplantation of an alginate–matrigel matrix containing isolated ovarian cells: first step in developing a biodegradable scaffold to transplant isolated preantral follicles and ovarian cells," *Biomaterials*, vol. 33, no. 26, pp. 6079–6085, 2012.
- [49] A. D. Augst, H. J. Kong, and D. J. Mooney, "Alginate hydrogels as biomaterials," *Macromolecular bioscience*, vol. 6, no. 8, pp. 623–633, 2006.
- [50] V. Breguet, U. v. Stockar, and I. W. Marison, "Characterization of alginate lyase activity on liquid, gelled, and complexed states of alginate," *Biotechnology progress*, vol. 23, no. 5, pp. 1223–1230, 2007.
- [51] N. C. Hunt, A. M. Smith, U. Gbureck, R. Shelton, and L. Grover, "Encapsulation of fibroblasts causes accelerated alginate hydrogel degradation," *Acta biomaterialia*, vol. 6, no. 9, pp. 3649–3656, 2010.

- [52] E. Alsberg, H. Kong, Y. Hirano, M. Smith, A. Albeiruti, and D. Mooney, "Regulating bone formation via controlled scaffold degradation," *Journal of dental research*, vol. 82, no. 11, pp. 903–908, 2003.
- [53] C. A. Simmons, E. Alsberg, S. Hsiong, W. J. Kim, and D. J. Mooney, "Dual growth factor delivery and controlled scaffold degradation enhance in vivo bone formation by transplanted bone marrow stromal cells," *Bone*, vol. 35, no. 2, pp. 562–569, 2004.
- [54] H. J. Kong, D. Kaigler, K. Kim, and D. J. Mooney, "Controlling rigidity and degradation of alginate hydrogels via molecular weight distribution," *Biomacromolecules*, vol. 5, no. 5, pp. 1720–1727, 2004.
- [55] K. Y. Lee and D. J. Mooney, "Alginate: properties and biomedical applications," *Progress in polymer science*, vol. 37, no. 1, pp. 106–126, 2012.
- [56] H. Lee, S. Fisher, M. S. Kallos, and C. J. Hunter, "Optimizing gelling parameters of gellan gum for fibrocartilage tissue engineering," *Journal of Biomedical Materials Research Part B: Applied Biomaterials*, vol. 98, no. 2, pp. 238–245, 2011.
- [57] S. H. Jahromi, L. M. Grover, J. Z. Paxton, and A. M. Smith, "Degradation of polysaccharide hydrogels seeded with bone marrow stromal cells," *Journal of the mechanical behavior of biomedical materials*, vol. 4, no. 7, pp. 1157–1166, 2011.
- [58] B. Luttrell, "The biological relevance of the binding of calcium ions by inositol phosphates," *Journal of Biological Chemistry*, vol. 268, no. 3, pp. 1521–1524, 1993.
- [59] D. F. Coutinho, S. V. Sant, H. Shin, J. T. Oliveira, M. E. Gomes, N. M. Neves, A. Khademhosseini, and R. L. Reis, "Modified gellan gum hydrogels with tunable physical and mechanical properties," *Biomaterials*, vol. 31, no. 29, pp. 7494–7502, 2010.
- [60] J. T. Oliveira, T. C. Santos, L. Martins, R. Picciochi, A. P. Marques, A. G. Castro, N. M. Neves, J. F. Mano, and R. L. Reis, "Gellan gum injectable hydrogels for cartilage tissue engineering applications: in vitro studies and preliminary in vivo evaluation," *Tissue Engineering Part A*, vol. 16, no. 1, pp. 343–353, 2009.
- [61] M. C. Koetting, J. T. Peters, S. D. Steichen, and N. A. Peppas, "Stimulus-responsive hydrogels: Theory, modern advances, and applications," *Materials Science and Engineering: R: Reports*, vol. 93, pp. 1–49, 2015.

- [62] J. Dissemond, M. Witthoff, T. Brauns, D. Haberer, and M. Goos, “ph values in chronic wounds. evaluation during modern wound therapy. (ph-wert des milieus chronischer wunden),” *Der Hautarzt; Zeitschrift fur Dermatologie, Venerologie, und verwandte Gebiete*, vol. 54, no. 10, pp. 959–965, 2003.
- [63] D. Schmaljohann, “Thermo-and ph-responsive polymers in drug delivery,” *Advanced drug delivery reviews*, vol. 58, no. 15, pp. 1655–1670, 2006.
- [64] J. Wu and M. J. Sailor, “Chitosan hydrogel-capped porous sio2 as a ph responsive nano-valve for triggered release of insulin,” *Advanced functional materials*, vol. 19, no. 5, pp. 733–741, 2009.
- [65] H. Zhang, S. Mardiyani, W. C. Chan, and E. Kumacheva, “Design of biocompatible chitosan microgels for targeted ph-mediated intracellular release of cancer therapeutics,” *Biomacromolecules*, vol. 7, no. 5, pp. 1568–1572, 2006.
- [66] J. F. Bradbeer, R. Hancocks, F. Spyropoulos, and I. T. Norton, “Low acyl gellan gum fluid gel formation and their subsequent response with acid to impact on satiety,” *Food hydrocolloids*, vol. 43, pp. 501–509, 2015.
- [67] J. F. Bradbeer, R. Hancocks, F. Spyropoulos, and I. T. Norton, “Self-structuring foods based on acid-sensitive low and high acyl mixed gellan systems to impact on satiety,” *Food hydrocolloids*, vol. 35, pp. 522–530, 2014.
- [68] I. Norton, W. Frith, and S. Ablett, “Fluid gels, mixed fluid gels and satiety,” *Food hydrocolloids*, vol. 20, no. 2, pp. 229–239, 2006.
- [69] C. Hoad, P. Rayment, R. Spiller, L. Marciani, B. C. Alonso, C. Traynor, D. Mela, H. Peters, and P. Gowland, “In vivo imaging of intragastric gelation and its effect on satiety in humans.” *The Journal of nutrition*, vol. 134, no. 9, pp. 2293–2300, 2004.
- [70] N. C. Hunt and L. M. Grover, “Cell encapsulation using biopolymer gels for regenerative medicine,” *Biotechnology letters*, vol. 32, no. 6, pp. 733–742, 2010.
- [71] N. C. Hunt, R. M. Shelton, and L. Grover, “An alginate hydrogel matrix for the localised delivery of a fibroblast/keratinocyte co-culture,” *Biotechnology journal*, vol. 4, no. 5, pp. 730–737, 2009.
- [72] N. C. Hunt, R. M. Shelton, and L. M. Grover, “Reversible mitotic and metabolic inhibition following the encapsulation of fibroblasts in alginate hydrogels,” *Biomaterials*, vol. 30, no. 32, pp. 6435–6443, 2009.

- [73] A. M. Smith, N. C. Hunt, R. M. Shelton, G. Birdi, and L. M. Grover, "Alginate hydrogel has a negative impact on in vitro collagen 1 deposition by fibroblasts," *Biomacromolecules*, vol. 13, no. 12, pp. 4032–4038, 2012.
- [74] Y. Han, T. Bai, and W. Liu, "Controlled heterogeneous stem cell differentiation on a shape memory hydrogel surface," *Scientific reports*, vol. 4, 2014.
- [75] L. M. G. Jennifer Z. Paxton, Fotios Spyropoulos, "Fluid gels as cell-carrying matrices: a potential method for burn wound regeneration," unpublished poster presentation.
- [76] W. J. Leo, A. J. McLoughlin, and D. M. Malone, "Effects of sterilization treatments on some properties of alginate solutions and gels," *Biotechnology progress*, vol. 6, no. 1, pp. 51–53, 1990.
- [77] S. Ohlson, P.-O. Larsson, and K. Mosbach, "Steroid transformation by living cells immobilized in calcium alginate," *European journal of applied microbiology and biotechnology*, vol. 7, no. 2, pp. 103–110, 1978. [Online]. Available: <http://dx.doi.org/10.1007/BF00505015>
- [78] R. H. McDowell, *Properties of alginates*, 4th ed. London: Alginate Industries, 1977.
- [79] D. Daigle and P. Cotty, "The effect of sterilization, ph, filler and spore inoculum concentration on the preparation of alginate pellets," *Biocontrol Science and Technology*, vol. 7, no. 1, pp. 3–10, 1997.
- [80] A. Rozier, C. Mazuel, J. Grove, and B. Plazonnet, "Functionality testing of gellan gum, a polymeric excipient material for ophthalmic dosage forms," *International journal of Pharmaceutics*, vol. 153, no. 2, pp. 191–198, 1997.
- [81] J. Holton, M. Imam, J. Ward, and M. Snow, "The basic science of bone marrow aspirate concentrate in chondral injuries," *Orthopedic Reviews*, vol. 8, no. 3, 2016.
- [82] J. Chahla, C. S. Dean, G. Moatshe, C. Pascual-Garrido, R. S. Cruz, and R. F. LaPrade, "Concentrated bone marrow aspirate for the treatment of chondral injuries and osteoarthritis of the knee a systematic review of outcomes," *Orthopaedic journal of sports medicine*, vol. 4, no. 1, p. 2325967115625481, 2016.
- [83] J. Holton, M. Imam, and M. Snow, "Bone marrow aspirate in the treatment of chondral injuries," *Frontiers in Surgery*, vol. 3, p. 33, 2016.

- [84] J. I. Dawson, J. O. Smith, A. Aarvold, J. N. Ridgway, S. J. Curran, D. G. Dunlop, and R. O. Oreffo, "Enhancing the osteogenic efficacy of human bone marrow aspirate: concentrating osteoprogenitors using wave-assisted filtration," *Cytotherapy*, vol. 15, no. 2, pp. 242–252, 2013.
- [85] Q. Zhao, S. Wang, J. Tian, L. Wang, S. Dong, T. Xia, and Z. Wu, "Combination of bone marrow concentrate and pga scaffolds enhance bone marrow stimulation in rabbit articular cartilage repair," *Journal of Materials Science: Materials in Medicine*, vol. 24, no. 3, pp. 793–801, 2013.
- [86] K. Mithoefer, L. Peterson, M. Zenobi-Wong, and B. R. Mandelbaum, "Cartilage issues in football—today's problems and tomorrow's solutions," *British journal of sports medicine*, vol. 49, no. 9, pp. 590–596, 2015.
- [87] J. M. Cassano, J. G. Kennedy, K. A. Ross, E. J. Fraser, M. B. Goodale, and L. A. Fortier, "Bone marrow concentrate and platelet-rich plasma differ in cell distribution and interleukin 1 receptor antagonist protein concentration," *Knee Surgery, Sports Traumatology, Arthroscopy*, pp. 1–10, 2016.
- [88] R. Mascarenhas, B. M. Saltzman, L. A. Fortier, and B. J. Cole, "Role of platelet-rich plasma in articular cartilage injury and disease," *Journal of Knee Surgery*, vol. 28, no. 01, pp. 003–010, 2015.
- [89] Y. Hou, C. H. Ryu, J. Jun, S. M. Kim, C. H. Jeong, and S.-S. Jeun, "Il-8 enhances the angiogenic potential of human bone marrow mesenchymal stem cells by increasing vascular endothelial growth factor," *Cell biology international*, vol. 38, no. 9, pp. 1050–1059, 2014.
- [90] L. A. Fortier, J. U. Barker, E. J. Strauss, T. M. McCarrel, and B. J. Cole, "The role of growth factors in cartilage repair," *Clinical Orthopaedics and Related Research®*, vol. 469, no. 10, pp. 2706–2715, 2011.
- [91] N. Zhou, Q. Li, X. Lin, N. Hu, J.-Y. Liao, L.-B. Lin, C. Zhao, Z.-M. Hu, X. Liang, W. Xu *et al.*, "Bmp2 induces chondrogenic differentiation, osteogenic differentiation and endochondral ossification in stem cells," *Cell and tissue research*, vol. 366, no. 1, pp. 101–111, 2016.
- [92] J. Pasold, K. Zander, B. Heskamp, C. Grüttner, F. Lüthen, T. Tischer, A. Jonitz-Heincke, and R. Bader, "Positive impact of igf-1-coupled nanoparticles on the differentiation potential of human chondrocytes cultured on collagen scaffolds," *International journal of nanomedicine*, vol. 10, p. 1131, 2015.

- [93] L. M. Mullen, S. M. Best, S. Ghose, J. Wardale, N. Rushton, and R. E. Cameron, "Bioactive igf-1 release from collagen-gag scaffold to enhance cartilage repair in vitro," *Journal of Materials Science: Materials in Medicine*, vol. 26, no. 1, pp. 1–8, 2015.
- [94] E. Moore, A. Bendele, D. Thompson, A. Littau, K. Waggle, B. Reardon, and J. Ellsworth, "Fibroblast growth factor-18 stimulates chondrogenesis and cartilage repair in a rat model of injury-induced osteoarthritis," *Osteoarthritis and Cartilage*, vol. 13, no. 7, pp. 623–631, 2005.
- [95] D. Correa, R. A. Somoza, P. Lin, S. Greenberg, E. Rom, L. Duesler, J. F. Welter, A. Yayan, and A. I. Caplan, "Sequential exposure to fibroblast growth factors (fgf) 2, 9 and 18 enhances hmsc chondrogenic differentiation," *Osteoarthritis and Cartilage*, vol. 23, no. 3, pp. 443–453, 2015.
- [96] H. Chuma, H. Mizuta, S. Kudo, K. Takagi, and Y. Hiraki, "One day exposure to fgf-2 was sufficient for the regenerative repair of full-thickness defects of articular cartilage in rabbits," *Osteoarthritis and cartilage*, vol. 12, no. 10, pp. 834–842, 2004.
- [97] C. Marchand, R. Williams, L. Grover, and M. Snow, "In vitro evaluation and optimized methodology to combine bone marrow aspirate concentrate with bst-cargel® as a new injectable treatment for cartilage repair," *Osteoarthritis and Cartilage*, vol. 23, p. A145, 2015.
- [98] V. Hegde, O. Shonuga, S. Ellis, A. Fragomen, J. Kennedy, V. Kudryashov, and J. M. Lane, "A prospective comparison of 3 approved systems for autologous bone marrow concentration demonstrated nonequivalency in progenitor cell number and concentration," *Journal of orthopaedic trauma*, vol. 28, no. 10, pp. 591–598, 2014.
- [99] M. S. Shive, C. D. Hoemann, A. Restrepo, M. B. Hurtig, N. Duval, P. Ranger, W. Stanish, and M. D. Buschmann, "Bst-cargel: in situ chondroinduction for cartilage repair," *Operative Techniques in Orthopaedics*, vol. 16, no. 4, pp. 271–278, 2006.
- [100] M. S. Shive, W. D. Stanish, R. McCormack, F. Forriol, N. Mohtadi, S. Pelet, J. Desnoyers, S. Méthot, K. Vehik, and A. Restrepo, "Bst-cargel® treatment maintains cartilage repair superiority over microfracture at 5 years in a multicenter randomized controlled trial," *Cartilage*, vol. 6, no. 2, pp. 62–72, 2015.
- [101] C. Hoemann, J. Sun, A. Legare, M. McKee, and M. Buschmann, "Tissue engineering of cartilage using an injectable and adhesive chitosan-based cell-delivery vehicle," *Osteoarthritis and cartilage*, vol. 13, no. 4, pp. 318–329, 2005.

- [102] N. Kohli, “An investigation of primary human cell sources and clinical scaffolds for articular cartilage repair,” Ph.D. dissertation, Aston University, 2016.
- [103] N. Kohli, K. T. Wright, R. L. Sammons, L. Jeys, M. Snow, and W. E. Johnson, “An in vitro comparison of the incorporation, growth, and chondrogenic potential of human bone marrow versus adipose tissue mesenchymal stem cells in clinically relevant cell scaffolds used for cartilage repair,” *Cartilage*, p. 1947603515589650, 2015.
- [104] S. Anders, M. Volz, H. Frick, and J. Gellissen, “A randomized, controlled trial comparing autologous matrix-induced chondrogenesis (amic®) to microfracture: analysis of 1-and 2-year follow-up data of 2 centers,” *The open orthopaedics journal*, vol. 7, no. 1, 2013.
- [105] O. Haddo, S. Mahroof, D. Higgs, L. David, J. Pringle, M. Bayliss, S. Cannon, and T. Briggs, “The use of chondrograde membrane in autologous chondrocyte implantation,” *The Knee*, vol. 11, no. 1, pp. 51–55, 2004.
- [106] G. Filardo, E. Kon, A. Roffi, A. Di Martino, and M. Marcacci, “Scaffold-based repair for cartilage healing: a systematic review and technical note,” *Arthroscopy: The Journal of Arthroscopic & Related Surgery*, vol. 29, no. 1, pp. 174–186, 2013.
- [107] G. P. Whyte, A. Gobbi, and B. Sadlik, “Dry arthroscopic single-stage cartilage repair of the knee using a hyaluronic acid-based scaffold with activated bone marrow-derived mesenchymal stem cells,” *Arthroscopy techniques*, vol. 5, no. 4, pp. e913–e918, 2016.
- [108] J. D. Wylie, M. K. Hartley, A. L. Kapron, S. K. Aoki, and T. G. Maak, “What is the effect of matrices on cartilage repair? a systematic review,” *Clinical Orthopaedics and Related Research®*, vol. 473, no. 5, pp. 1673–1682, 2015.
- [109] M. Spoliti, P. Iudicone, R. Leone, A. De Rosa, F. R. Rossetti, and L. Pierelli, “In vitro release and expansion of mesenchymal stem cells by a hyaluronic acid scaffold used in combination with bone marrow,” *Muscles, Ligaments and Tendons Journal*, vol. 2, no. 4, p. 289, 2012.
- [110] J. Zeltinger, J. K. Sherwood, D. A. Graham, R. Müller, and L. G. Griffith, “Effect of pore size and void fraction on cellular adhesion, proliferation, and matrix deposition,” *Tissue engineering*, vol. 7, no. 5, pp. 557–572, 2001.
- [111] S. Gunasekaran and M. M. Ak, “Dynamic oscillatory shear testing of foods-selected applications,” *Trends in Food Science & Technology*, vol. 11, no. 3, pp. 115–127, 2000.

- [112] C. Yan and D. J. Pochan, "Rheological properties of peptide-based hydrogels for biomedical and other applications," *Chemical Society Reviews*, vol. 39, no. 9, pp. 3528–3540, 2010.
- [113] N. C. Hunt, "An alginate hydrogel matrix for the localised delivery of a fibroblast/keratinocyte co-culture to expedite wound healing," Ph.D. dissertation, University of Birmingham, 2010.
- [114] R. Moakes, A. Sullo, and I. Norton, "Preparation and characterisation of whey protein fluid gels: The effects of shear and thermal history," *Food Hydrocolloids*, vol. 45, pp. 227–235, 2015.
- [115] I. F. Farrés, M. Douaire, and I. Norton, "Rheology and tribological properties of ca-alginate fluid gels produced by diffusion-controlled method," *Food Hydrocolloids*, vol. 32, no. 1, pp. 115–122, 2013.
- [116] O. Behnke, "Electron microscopical observations on the surface coating of human blood platelets," *Journal of ultrastructure research*, vol. 24, no. 1, pp. 51–69, 1968.
- [117] W. L. Stoppel, J. C. White, S. D. Horava, A. C. Henry, S. C. Roberts, and S. R. Bhatia, "Terminal sterilization of alginate hydrogels: efficacy and impact on mechanical properties," *Journal of Biomedical Materials Research Part B: Applied Biomaterials*, vol. 102, no. 4, pp. 877–884, 2014.
- [118] M. Murata, K. Yudoh, and K. Masuko, "The potential role of vascular endothelial growth factor (vegf) in cartilage: how the angiogenic factor could be involved in the pathogenesis of osteoarthritis?" *Osteoarthritis and cartilage*, vol. 16, no. 3, pp. 279–286, 2008.
- [119] A. G. Håti, D. C. Bassett, J. M. Ribe, P. Sikorski, D. A. Weitz, and B. T. Stokke, "Versatile, cell and chip friendly method to gel alginate in microfluidic devices," *Lab on a Chip*, vol. 16, no. 19, pp. 3718–3727, 2016.